1969

# Threshold characteristics of frequency modulation noise

Charles J. Ludinsky
*Lehigh University*

# THRESHOLD CHARACTERISTICS

# OF FREQUENCY MODULATION NOISE

by

Charles J. Ludinsky

A Thesis

Presented to the Graduate Faculty

of Lehigh University

in Candidacy for the Degree of

Master of Science

Lehigh University

1969

This thesis is accepted and approved in partial fulfillment of the requirements for the degree of Master of Science.

10 MARCH 1969
(date)

John Andrea
Professor in charge

A. K. Fuhrhird
Head of the Department

## ACKNOWLEDGEMENT

I would like to thank Dr. John G. Ondria for his guidance and assistance given to me.

I would also like to express my gratitude to Bell Telephone Laboratories for their support in making this Graduate Study possible and for the use of their facilities.

Finally, I would like to thank my wife, Barbara, for her patience and encouragement.

# TABLE OF CONTENTS

# LIST OF TABLES AND FIGURES

# ABSTRACT

This paper presents a study of the behavior of an FM system with carrier-to-noise ratios in the threshold region. Although work has been done to determine the long-term average signal-to-noise ratio of the receiver and the output noise spectrum, this study was directed toward determination of the statistical distribution of the noise output.

The nonlinear nature of frequency modulation plus the statistical character of random noise provide a problem which is not subject to any simple analysis. Recent work by S. O. Rice and other investigators has provided some understanding of the behavior of FM systems near threshold. The methods used provide approximations to various output parameters, plus some insight to the nature of the output distribution. A brief explanation of some previous works and their application to an understanding of the statistical properties of FM receiver noise is included.

The use of computer simulations often simplify problem solutions and provide a closer approximation to the real case. This method is suggested in the study of FM noise. The method utilizes a phasor representation of carrier plus noise, considering only the unmodulated carrier case. It can be extended, without much change, to include the case of a modulated carrier.

An experimental study of FM receiver noise in the threshold region is included. This study also involves the use of an unmodulated carrier. The system used FM-FDM (frequency division multiplex) equipment. The output noise distribution is determined for three channel slots of the system and for various carrier-to-noise ratios in the threshold region.

## I. Introduction

A necessary prerequisite for the proper utilization of a communications system is a thorough knowledge of the noise properties of the system. Such a knowledge enables one to effect a useful separation of information from noise when the system exhibits a low carrier-to-noise ratio. The use of such knowledge is apparent in applications involving space vehicles where long distances and low transmitter powers necessitate receiver optimization techniques. A similar need exists for many earthbound communications systems where economic limitations place the design emphasis on the receiving end.

Some of the original investigators of FM system properties demonstrated, both experimentally and analytically, the signal-to-noise ratio improvement characteristics for wideband FM.[1,2] It was soon noted, however, that the predicted improvement did not exist for all carrier-to-noise ratios. It was found that the improvement was relatively constant until the carrier-to-noise ratio was reduced to a certain "threshold" region. A further reduction in carrier-to-noise ratio then resulted in a rapid deterioration of signal-to-noise ratio. Later investigation showed that the threshold conditions occurred with a carrier-to-noise ratio of approximately 10 db.[3,4,5]

The noise output from an FM system has a Gaussian distribution when the carrier-to-noise ratio is either very large (i.e., >10 db) or very small (i.e., <<0 db) and the input noise also has a Gaussian distribution. This was shown analytically by later investigators.[3,4,5] However, in the region of threshold

the noise output was thought to have a non-Gaussian distribution. This idea originated by experiments near threshold. It was found that the noise contained excess large amplitude excursions; that is, such levels occur with a greater probability than predicted by a Gaussian distribution with the same rms value.

The purpose of this study was to explain the behavior of an FM system near the threshold region and to provide a qualitative discussion of the output distribution. The method used involves an extension of the phasor representation of carrier and noise used in many discussions on this subject and developed early in the study of FM noise.

A real system consisting of FM-FDM (frequency division multiplex) equipment was also used to determine experimentally the noise distribution in the threshold region. These investigations cover the range of carrier-to-noise ratios from -4 db to +18 db.

## II. Statistical Properties of Random Noise

Narrowband random noise can be represented as a sine wave of center frequency $\omega_o$ varying both in amplitude and phase.[6,7] The corresponding noise current can be represented as

$$I_N(t) = R(t)\cos[\omega_o t + \phi(t)] \qquad (2.1)$$

where R(t) is its time varying amplitude, $\phi(t)$ its instantaneous phase variation, and $\omega_o$ is the center (angular) frequency.

The amplitude R(t) has a Rayleigh distribution; hence, the probability density function is

$$p(R) = \frac{R}{\sigma^2} e^{-R^2/2\sigma^2} \qquad (2.2)$$

where $\sigma$ represents the standard deviation and the rms value of the noise.[6,7]

The phase, $\phi(t)$, is completely random. This means that for an observation at any instant of time, the angle associated with the noise phasor can have any value from 0 to $2\pi$ with equal probability, i.e.,

$$p(\phi) = \frac{1}{2\pi}; \quad 0 \leq \phi < 2\pi. \qquad (2.3)$$

Narrowband random noise can also be represented by in-phase and quadrature components. For a noise current

$$I_N(t) = x(t)\cos \omega_o t + y(t)\sin \omega_o t \qquad (2.4)$$

where $x(t)$ and $y(t)$ are independent Gaussian variables and $\omega_o$ is the center frequency. The corresponding probability density functions are

$$p(x) = \frac{1}{\sqrt{2\pi}\ \sigma} e^{-\frac{1}{2}\frac{x^2}{\sigma^2}} \qquad (2.5)$$

$$p(y) = \frac{1}{\sqrt{2\pi}\ \sigma} e^{-\frac{1}{2}\frac{y^2}{\sigma^2}}.$$

Equivalence between the two representations can be shown as follows. If $x(t)$ and $y(t)$ are considered as the rectangular coordinates of a random point M on a plane, then the probability that this point will fall within an infinitely thin ring contained between the circles of radius R and R + dR is determined by the equality

$$P(R \leq r \leq R + dR) = \iint_{R \leq \sqrt{x^2+y^2} \leq R + dR} p(x,y)dx\ dy \qquad (2.6)$$

where

$$p(x,y) = p(x)p(y) = \frac{1}{2\pi\sigma^2} e^{-\frac{1}{2\sigma^2}(x^2+y^2)}.$$

Changing from rectangular to polar coordinates:

$$p(R)dR = \frac{1}{2\pi\sigma^2} \int_R^{R+dR} \int_0^{2\pi} e^{-r^2/2\sigma^2} r d\phi dr. \qquad (2.7)$$

Integrating and dividing by dR

$$p(R) = \frac{R}{\sigma^2} e^{-R^2/2\sigma^2} \qquad (2.8)$$

results. The absence of the phase term $\phi$ from the integrand in eq. (2.7) means the distribution of $\phi(t)$ is uniform.

An additional representation of narrowband noise, from which the preceding may be derived, is also possible.[6,8] Consider a time period T during which observations are made. Let x(t) represent the noise amplitude for $0 < t < T$. A Fourier series of the form

$$x(t) = \sum_{n=1}^{\infty} (x_{cn} \cos \omega_n t + x_{sn} \sin \omega_n t) \qquad (2.9)$$

may be written, where

$$\omega_n = 2\pi n/T$$

$$x_{cn} = \frac{2}{T}\int_0^T x(t)\cos\ \omega_n t\ dt$$

and

$$x_{sn} = \frac{2}{T}\int_0^T x(t)\sin\ \omega_n t\ dt.$$

For a Gaussian noise process $x_{cn}$ and $x_{sn}$ are Gaussian random variables which become statistically uncorrelated as the interval T increases without limit. That is

$$\lim_{T\to\infty} \overline{x_{cn}x_{sn}} = 0.$$

Writing $\omega_n = (\omega_n - \omega_o) + \omega_o$, where $\omega_o$ is the radian center frequency of the narrowband random noise process, substituting this into the Fourier series representation and expanding the factors yields

$$x(t) = x_c(t)\cos\ \omega_o t - x_s(t)\sin\ \omega_o t \qquad (2.10)$$

where

$$x_c(t) = \sum_{n=1}^{\infty} [x_{cn}\cos(\omega_n-\omega_o)t + x_{sn}\sin(\omega_n-\omega_o)t] \quad (2.11)$$

$$x_s(t) = \sum_{n=1}^{\infty} [x_{cn}\sin(\omega_n-\omega_o)t - x_{sn}\cos(\omega_n-\omega_o)t] \quad (2.12)$$

Since $x_c(t)$ and $x_s(t)$ consist of a sum of Gaussian variates they are also Gaussian variates. From eqs. (2.11) and (2.12) the result

$$\lim_{T\to\infty} \overline{x_c(t)x_s(t)} = 0$$

is obtained. For a noise current eq. (2.4) is similar to eq. (2.10) where $x_c(t) = x(t)$ and $x_s(t) = y(t)$.

## III. Threshold Characteristics

The signal-to-noise ratio improvement characteristics of wideband FM were demonstrated experimentally by E. H. Armstrong in 1936.[1] The following year M. G. Crosby published a paper[2] showing analytically and experimentally similar results. Crosby also demonstrated the existence of the improvement threshold.

The term, signal-to-noise ratio, is taken here as the ratio of mean signal power to mean noise power.

To determine the improvement characteristics we begin by assuming an ideal FM receiver consisting of an ideal rectangular bandpass IF amplifier of bandwidth 2B Hz, an ideal limiter which removes all amplitude variations, an ideal discriminator with an output voltage directly proportional to the instantaneous frequency, and an ideal low-pass filter of bandwidth $f_m$ Hz where $f_m$ is the maximum frequency of the modulating signal and $f_m < B$.[9,10]

Assuming a modulation signal of the form

$$f(t) = \frac{\Delta\omega}{2\pi} \cos \omega_k t; \quad \omega_k \leq \omega_m \tag{3.1}$$

where $\Delta\omega/2\pi$ represents the maximum frequency deviation of the carrier, the frequency modulated carrier at the output of the IF amplifier, in the absence of noise, is

$$v_c(t) = A_c \cos\left(\omega_c t + \frac{\omega_m}{\omega_k} \beta \sin \omega_k t\right) \qquad (3.2)$$

where $\beta = \Delta\omega/\omega_m$ is the modulation index.

The average power of the FM wave is

$$S_c = \frac{1}{2} A_c^2 \qquad (3.3)$$

and is independent of the modulation. The instantaneous frequency

$$\omega_i = \frac{d\theta(t)}{dt} = \omega_c + \beta\omega_m \cos \omega_k t = \omega_c + \Delta\omega \cos \omega_k t \qquad (3.4)$$

where $\theta$ is the phase of $v_c(t) = A_c \cos \theta(t)$. The output from the discriminator is proportional to the instantaneous frequency, i.e.,

$$v(t) = b\Delta\omega \cos \omega_k t \qquad (3.5)$$

where b is a proportionality constant of the discriminator.

The discriminator output is then filtered to remove undesired high-frequency terms. The filter is designed to pass only the modulation frequency components. For this case it would have a bandpass of $f_m$ Hz.

From eq. (3.5) the average output power is

$$S_o = \frac{b^2(\Delta\omega)^2}{2} \qquad (3.6)$$

assuming a normalized load.

To determine the output noise power, assume an unmodulated carrier plus noise. Assume the noise has a spectral density of z watts/Hz, uniformly distributed throughout the 2B Hz bandwidth of the IF amplifier. Using a noise representation consisting of a discrete number of sine waves each having equal amplitude and arbitrary phase and spaced df Hz apart, the noise component at frequency $f_c + f$ is

$$N(t) = A_n \cos(\omega_c+\omega)t \qquad (3.7)$$

and

$$\frac{A_n^2}{2} = z\ df. \qquad (3.8)$$

Adding the noise term to the unmodulated carrier, the output voltage of the IF amplifier becomes

$$A_n \cos(\omega_c+\omega)t + A_c \cos\ \omega_c t = A(t)\cos[\omega_c t + \theta(t)] \qquad (3.9)$$

where

$$\theta(t) = \tan^{-1}\left[\frac{A_n \sin \omega t}{A_c + A_n \cos \omega t}\right]. \qquad (3.10)$$

After limiting, a constant amplitude phase modulated signal voltage

$$A \cos[\omega_c t + \theta(t)] \qquad (3.11)$$

results.

When $A_c >> A_n$ (i.e., large carrier-to-noise ratio)

$$\theta(t) \approx \frac{A_n}{A_c} \sin \omega t \qquad (3.12)$$

and the output from the limiter is

$$A \cos\left[\omega_c t + \frac{A_n}{A_c} \sin \omega t\right] \qquad (3.13)$$

which is the form of a narrowband FM signal with $\beta = A_n/A_c << 1$.

From eq. (3.12) the discriminator noise output is

$$v_D(t) = b \frac{d\theta(t)}{dt} = b\omega \frac{A_n}{A_c} \cos \omega t, \qquad (3.14)$$

i.e., the output of the discriminator is proportional to the frequency difference between the noise term and the carrier. The power output due to the noise component is

$$dN_o = \frac{1}{2}\left(b\omega\,\frac{A_n}{A_c}\right)^2 = \left(\frac{b\omega}{A_c}\right)^2 \frac{A_n^2}{2} \qquad (3.15)$$

or

$$dN_o = \left(\frac{b\omega}{A_c}\right)^2 z\ df.$$

Hence

$$\frac{dN_o}{df} = \left(\frac{b\omega}{A_c}\right)^2 z \qquad (3.16)$$

is the power spectral density of FM noise at the discriminator output. The total noise power at the low-pass filter output is

$$N_o = z\left(\frac{b}{A_c}\right)^2 \int_{-f_m}^{f_m} \omega^2 df \qquad (3.17)$$

where f is integrated from $-f_m$ to $f_m$ to include the power from both sidebands. After integration

$$N_o = \frac{2z}{3}\left(\frac{2\pi b}{A_c}\right)^2 f_m^3 = \frac{2z}{3}\frac{b^2\omega_m^2}{A_c^2} f_m \qquad (3.18)$$

and since $\frac{A_c^2}{2} = S_c$

$$N_o = \frac{zb^2}{3S_c}\omega_m^2 f_m. \qquad (3.19)$$

From eq. (3.6), the mean S/N power ratio at the output is

$$\frac{S_o}{N_o} = 3\left(\frac{\Delta\omega}{\omega_m}\right)^2 \frac{S_c}{2zf_m}. \qquad (3.20)$$

Since $2zf_m = N_c$, the total noise power in the AM sidebands, and $\beta = \Delta\omega/\omega_m$

$$\frac{S_o}{N_o} = 3\beta^2 \frac{S_c}{N_c}. \qquad (3.21)$$

This is the result, developed by Crosby, showing the effective signal-to-noise ratio as a function of the modulation index.

As the carrier power is reduced the assumptions required for the previous derivation become inapplicable. At some point the total noise power will equal the carrier power,

and the approximation $A_c >> A_n$ will no longer be valid. In fact, $A_n$ begins to exceed $A_c$ a significant number of times before the carrier-to-noise ratio drops to 0 db. Taking 1 percent as a significant figure for the number of times $|A_n|$ exceeds $|A_c|$, the carrier-to-noise ratio can be determined at that point. Assuming Gaussian noise at the IF

$$.99 = \frac{1}{\sqrt{2\pi}\,\sigma} \int_{-A_c}^{A_c} e^{-x^2/2\sigma^2} dx, \quad \sigma^2 = N_c,$$

from which $A_c \simeq 2.58\sigma$. Then

$$\frac{S_c}{N_c} = \frac{A_c^2}{N_c} = (2.58)^2 = 6.65 = 8.2 \text{ db.}$$

This compares with the value of 10 db established experimentally as the beginning of the threshold region. Table (3.1) illustrates the significance of a small change in carrier-to-noise power ratio near threshold.

Table 3.1 - Effect of small changes in carrier-to-noise ratio near threshold.

| C/N db | Percent of Time $\lvert A_n \rvert > \lvert A_c \rvert$ |
|---|---|
| 11 | .04 |
| 10 | .18 |
| 8 | 1.21 |
| 6 | 4.6 |
| 4 | 11.4 |

The effect of noise near the threshold region can be best demonstrated by a method described by S. O. Rice.[11] Consider the phasor diagram of Fig. (3.1). With the carrier unmodulated we have the situation shown, where x(t) and y(t) represent the in-phase and quadrature components of $A_n(t)$, $|R(t)|$ represents the magnitude of the resultant vector, and $\theta(t)$ represents the instantaneous deviation angle. The radius of the circle Q is equal to $|A_n|$, the RMS value of the noise. Assume the radius of Q to be approximately 1/3 of $A_c$. This represents a carrier-to-noise power ratio of 9.5 db. About 68 percent of the time $A_n(t)$ will be inside of the circle Q. Occasionally $A_n(t)$ will exceed $A_c$. This might occur for any value of $\phi$. However, when this occurs at the same time that $\phi$ passes through $\Pi$ radians, $\theta$ changes by approximately $\pm 2\pi$ radians. The result is an impulse of area approximately $\pm 2\pi$ radians for $d\theta/dt$. When $A_n(t)$ is slightly less than $A_c$ and $\phi$ passes through $\pi$, the result for $d\theta/dt$ is two consecutive pulses of area approximately $\pi$ with opposite signs. These effects are illustrated in Fig. (3.2).

It can be seen in (b) that the discriminator output will contain very little low-frequency energy (i.e., the net area is approximately zero). Conversely, (a) exhibits a significant area; hence, low-frequency energy. Since the output from the discriminator is then passed through a low-pass filter only those pulses of area $\pm 2\pi$ contribute to the output. The result, for audio output equipment, is an

occasional pulse, or "click" (as termed by Rice). The remainder of the time the discriminator output, $d\theta/dt$, assumes a Gaussian form. The discriminator output may then be thought of as being composed of these two components. This idea is illustrated in Fig. (3.3).

The output from the low-pass filter can be qualitatively determined from the above. When the carrier-to-noise ratio is large, the click rate will be extremely small, and the output will appear Gaussian. As the ratio is reduced the average click occurrence frequency $f_{cl}$, will become significant when compared to $f_m$, where $f_m$ is the bandpass of the filter. This will result in a distribution containing a significant number of samples exceeding that predicted by the Gaussian distribution function. As the ratio is further reduced, $f_{cl} \rightarrow f_m$. In addition, other pulses of area $<2\pi$ contribute to the discriminator output. The filter output then assumes a Gaussian form, an effect established by the Central Limit Theorem.[7,12] These results are illustrated in Fig. (3.4).

These effects provide the base for the experiment and will be explained in detail in Section IV.

The power output from the bandpass filter is a function of the Gaussian noise current for high carrier-to-noise ratios. In the threshold region the clicks begin to contribute an additional power component. At some point the power from the clicks will equal the Gaussian component power. Further reduction in the carrier-to-noise ratio results in a rapid

increase in the number of clicks, and the power contributed by the clicks will greatly exceed the power of the Gaussian component. In a region below threshold, therefore, the power will be determined by the click rate. For very low carrier-to-noise ratios the discriminator output again assumes a Gaussian-type output.

Rice[4,11] showed that the click rate is given by the relation

$$N = r(1 - \mathrm{erf}\sqrt{\rho}) \qquad (3.22)$$

where $\rho$ is the ratio of average carrier power to average input noise power, and 2r is the expected number of zeros per second of the quadrature noise component. For a rectangular filter $r = B/\sqrt{12}$ where B is the bandwidth in Hertz. For a normal filter $r = \sigma$ where $\sigma$ is the standard deviation of the filter. Including the contributions from both the clicks and the Gaussian noise component, the output signal-to-noise ratio can then be shown to approximate the following (no modulation)

$$\frac{S_o}{N_o} = \frac{3\rho\beta^2(2f_m)^{-3}}{\rho\sqrt{3}\,(1 - \mathrm{erf}\sqrt{\rho})(\beta/f_m)^2 + 1} \qquad (3.23)$$

for a rectangular input filter. Here $S_o = \pi^2 B^2/2$ and $f_m$ is the cutoff frequency of the low-pass output filter. For a normal law bandpass filter the approximation becomes

$$\frac{S_o}{N_o} = \frac{3\rho B_e^2 (2f_m)^{-3}}{\rho(18\pi)^{1/2}(1 - \text{erf}\sqrt{\rho})(B_e/f_m)^2 + (1 - .3\sigma^{-2}f_m^2 + \ldots)} \qquad (3.24)$$

where $B_e = \sigma\sqrt{2\pi}$ is the equivalent rectangular bandwidth of the normal law (Gaussian) input filter, and $S_o = \pi^2 B_e^2/2$. The dependence of the output signal-to-noise ratio ($S_o/N_o$) on the input carrier-to-noise ratio is shown in Fig. (3.5).

A computer simulation analysis of the noise distribution problem is also possible. Consider a narrowband noise process with center frequency $f_c$ and bandwidth $B << f_c$. Representing the noise N(t) as

$$N(t) = \sum_{\omega_n > \omega_L}^{\omega_n < \omega_u} (a_n \cos \omega_n t + b_n \sin \omega_n t) \qquad (3.25)$$

where

$$\omega_n = \frac{2\pi}{T} n; \quad \omega_L = \omega_c - \frac{1}{2} B; \quad \omega_u = \omega_c + \frac{1}{2} B$$

and

$$n = 0,1,2,3,\ldots .$$

for a rectangular bandpass. The coefficients are normally distributed random numbers, easily generated in a computer program. T is a time period such that T >> 1/B. It should be selected to give a statistically significant time sample of the narrowband noise process (e.g., T = 10,000×1/B). The collection of coefficients then offers a reasonable representation of a time sample of narrowband random noise.

With the above, for the case of an unmodulated carrier plus noise, the input to an ideal limiter is

$$v(t) = A \cos \omega_c t + N(t) \tag{3.26}$$

where A is the carrier amplitude. From eq. (3.25) this becomes

$$v(t) = A \cos \omega_c t + \sum_{\omega_n > \omega_L}^{\omega_n < \omega_u} (a_n \cos \omega_n t + b_n \sin \omega_n t). \tag{3.27}$$

An equivalent representation is

$$v(t) = A \cos \omega_c t + \sum_{m=-M}^{M} [a_m \cos(\omega_c + \omega_m)t + b_m \sin(\omega_c + \omega_m)t] \tag{3.28}$$

where $\omega_m = \omega_c$ for m = 0 and $a_{-M}$ is equivalent to the first $a_n$, and $b_{-M}$ is equivalent to the first $b_n$, etc., for all $a_m$ and all $b_m$. Expanding,

$$v(t) = A \cos \omega_c t + \sum_{m=-M}^{M} [x_m(t)\cos \omega_c t + y_m(t)\sin \omega_c t] \tag{3.29}$$

where

$$x_m(t) = a_m \cos \omega_m t + b_m \sin \omega_m t, \tag{3.30}$$

$$y_m(t) = - a_m \sin \omega_m t + b_m \cos \omega_m t.$$

Equivalently

$$v(t) = \left[A + \sum_{m=-M}^{M} x_m(t)\right] \cos \omega_c t + \left[\sum_{m=-M}^{M} y_m(t)\right] \sin \omega_c t, \tag{3.31}$$

which is the quadrature and in-phase representation of a carrier plus narrowband random noise given by

$$v(t) = [A + x(t)]\cos \omega_c t + y(t)\sin \omega_c t \tag{3.32}$$

where x(t) and y(t) are the sums in the previous equation. The phasor diagram of Fig. (3.1) now applies.

The instantaneous phase is

$$\theta(t) = \tan^{-1} \frac{y(t)}{A + x(t)} \tag{3.33}$$

and

$$\dot{\theta}(t) = \frac{[A + x(t)]\dot{y}(t) - y(t)\dot{x}(t)}{A^2 + x^2(t) + y^2(t) + 2Ax(t)} \tag{3.34}$$

which is separable into a function of $\dot{x}(t)$ and a function of $\dot{y}(t)$. That is

$$\dot{\theta}(t) = P(t)\dot{y}(t) + S(t)\dot{x}(t). \tag{3.35}$$

The functions $x(t)$, $y(t)$, $\dot{x}(t)$ and $\dot{y}(t)$ are varying slowly in comparison with the center frequency $\omega_c$. $\dot{x}(t)$ and $\dot{y}(t)$ can be easily determined from $x(t)$ and $y(t)$, i.e.,

$$\dot{x}(t) = \frac{x\left(t + \frac{1}{2}h\right) - x\left(t - \frac{1}{2}h\right)}{h} \tag{3.36}$$

and

$$\dot{y}(t) = \frac{y\left(t + \frac{1}{2}h\right) - y\left(t - \frac{1}{2}h\right)}{h}$$

as reasonable approximations when $h << \frac{1}{B}$ . However, $h >> 1/f_c$ is also possible for a valid representation for $\dot{x}(t)$ and $\dot{y}(t)$. The actual value for h can be selected to give the desired accuracy.

The functions S(t) and P(t) are undefined when

$$A^2 + x^2(t) + y^2(t) + 2Ax(t) = 0$$

or (3.37)

$$[x(t) + A]^2 + y^2(t) = 0$$

i.e., $y(t) = 0$ and $x(t) = -A$. The behavior of P(t) and S(t) are given in Figs. (3.6) and (3.7) with A = 1.

Consider the circle defined by the equation

$$[x(t) + A]^2 + y^2(t) = .04A^2. \qquad (3.38)$$

Points outside of the circle result in values for P(t) and S(t) which vary slowly with x(t) and y(t). Points inside the circle, however, produce larger values for P(t) and S(t) and rapidly changing first derivatives, $\dot{P}(t)$ and $\dot{S}(t)$.

A two-part solution for a simulation analysis of the discriminator output is therefore necessary. For values of x(t) and y(t) which simultaneously occur outside of the circle defined above, time increments $\Delta t$ may be used, where

$\Delta t \approx 1/10B$. A smaller time increment must be used for points inside the circle if the discriminator output is to be reasonably approximated.

A somewhat easier approach may use the same method with a square area defined by the following

$$-.2A < y(t) < .2A$$

$$-1.2A < x(t) < -.8A. \tag{3.39}$$

It is therefore necessary to find the values of t which result in the ~~following~~

$$x(t) = \sum_{m=-M}^{M} x_m(t) = -A$$

and

$$y(t) = \sum_{m=-M}^{M} y_m(t) = 0$$

and to evaluate $x(t)$, $y(t)$, $\dot{x}(t)$, and $\dot{y}(t)$ for reduced time increments about these values for t until the interior of the square (or circular) area is covered.

No matter how small the time increment, an occasional impulse term may be lost. This occurs when $x(t) \rightarrow -A$

and $y(t) \to 0$ simultaneously. However, by selecting a reasonably small time increment, the loss can be reduced to an insignificant value. That is, the probability of the occurrence of a pulse with a period $<\Delta t$ decreases rapidly as $\Delta t \to 0$.

After compiling the large quantity of data resulting from the computations described, the discriminator output

$$\dot{\theta}(t) = P(t)\dot{y}(t) + S(t)\dot{x}(t) \qquad (3.35)$$

can be calculated where $t = t_o + n\Delta t$, $\Delta t$ is described above, n is the sample number, and $t_o$ is the beginning of the time period T. Then

$$T = \sum_{n=1}^{N} (t_o + n\Delta t_n).$$

Note that $\Delta t = \Delta t_n$ is not a constant. N is the total number of samples.

A more realistic result may be obtained by limiting the maximum value of $|\dot{\theta}(t)|$. This represents an approximation to a real discriminator.

The output of a real FM discriminator is passed through a bandpass or low-pass filter, and the filter output may be the end product of the system, i.e., the receiver output. The filter output can be determined from the filter characteristics and the calculated discriminator output.

## IV. Experimental Determination of Noise Distribution

The distribution of noise was determined in a 3 kHz voice channel slot of an FM-FDM system operating in the threshold region without modulation. The procedure followed was:

1. Calculation of input noise power.
2. Organization of a variable power carrier source.
3. Recording of data for various carrier to noise power ratios and various baseband slots.
4. Conversion of analog data to digital form.
5. Computer analysis of digital data.
6. Interpretation of computer results.

### Description of FM System Equipment

The major equipment used in the experimental system consisted of the modulation and demodulation units, a test multiplex system, and step attenuators to produce the desired carrier-to-noise power ratio.

The equipment associated with data recording and measuring included RF power meters, oscilloscope, analog data recorder, analog-digital data converter, and data processing equipment.

A detailed description of the individual component devices is given in the appendix.

The equipment arrangement is illustrated in Fig. (4.1).

### Determination of Carrier-to-Noise Power Ratios

The carrier-to-noise ratio is calculated by including the effects of thermal noise plus the noise contribution

of the input preamplifier. The thermal noise power is

$$P_T = kT\Delta f \text{ watts}$$

where k is Boltzman's constant, T is temperature in degrees Kelvin and $\Delta f$ is the effective IF bandwidth. For 20°C and an IF bandwidth of 3 MHz $P_T = 1.21\times10^{-14}$ watts (-109 dBm). The preamplifier has a noise figure of 7.9 dB, hence the effective input noise power is approximately -101 dBm.

The threshold occurs at a carrier-to-noise power ratio of approximately 10 dB. The carrier power at threshold would then be (-101+10) dBm = -91 dBm. The modulator provides a highly stable source of RF power at 70 MHz. With an unmodulated output set at -50 dBm (as measured with an RF power meter), the threshold carrier-to-noise ratio is achieved by attenuating the modulator output by 41 dB. Using a variable attenuator the carrier-to-noise ratio can be varied as desired about the threshold region. The range of C/N ratios were selected from 18 dB to -4 dB. This range extends from well above the threshold region to a point below the signal suppression (secondary) threshold.

Multiplex Equipment

The equipment used in the experiment was designed to carry 252 voice channels spaced at 4 kHz intervals. A

test multiplex was available which translates a 4 kHz voice channel into one of five positions in the baseband. The noise distribution with an unmodulated carrier was found in the three channel slots with center frequencies 70 kHz, 105 kHz and 290 kHz. The output from the DEMUX (demultiplexer) is passed through a 3 kHz low-pass filter (the 1 kHz difference providing a guard band). Since the carrier is unmodulated, the filter output contains only the effective noise in the baseband slot.

Data Recording

The noise level at the filtered output varies extensively with the carrier-to-noise input ratio. For a range of input C/N ratios from 18 dB to -4 dB, the average output noise power varies about 30 dB. The variation of noise power with input C/N ratio for the 70 kHz slot is shown in Fig. (4.2). The noise improvement threshold and the secondary or signal suppression threshold regions can be clearly seen. To facilitate recording and processing of data, it was necessary to attenuate the output to maintain a reasonable range of input levels to the recording and processing equipment.

The noise output, after attenuation, provided the input signal to an analog data recorder with an oscilloscope used as a monitor. A brief study indicated that the recorder saturated with an input of ±350 millivolts. To utilize the full capability of the recorder while avoiding processing

distortion, a maximum input level of ±300 millivolts was chosen. Since occasional large amplitude excursions could be expected, it was necessary to provide a somewhat arbitrary limit on the number of excursions per second exceeding the ±300 millivolt limit. A maximum limit of 1 excursion in a 5 second period was accepted. This was achieved by observing the noise on the oscilloscope and adjusting the output attenuation until the desired range was achieved.

The processing of the data provided another reason for limiting the range of input data. This will be explained subsequently.

The process of collecting the desired data proceeded as follows. A 10-second recording was made of a 1000 Hz, 600 mv p-p sine wave as a reference calibration signal. Similar 10-second recordings were made for each C/N ratio and each baseband slot. The 10-second recording time was used to provide several seconds for the recorder to reach proper speed and the remaining time interval for the acquisition of data. The tape was marked to locate the data and a 10-second blank spot was allowed between runs. In all, fifty-five 10-second runs were recorded for processing.

Data Processing

In order to determine the distribution of the output noise, the sampling theorem was utilized with the aid of an analog-to-digital converter. The A-D converter effectively measures a signal at certain time intervals determined by the

sampling rate, then provides a numerical value for each analog sample. In this case a sampling rate of 8000 samples per second was selected to provide a complete description of the 3000 Hz noise signal. A total of about 16,000-24,000 samples (2-3 seconds) was taken from each 10-second recorded run.

The characteristics of the computer program used to determine the distribution was the reason for maintaining a certain range on the recorded analog data. Once the data was converted to digital form, it was recorded on digital tape. The computer program then analyzed it as a discrete variable. 4095 discrete levels, varying from -300 mv to +300 mv were used to assort the data. That is, the number of samples with a value between $n\Delta v$ and $(n+1)\Delta v$ were counted, where $-(4095-1)/2 < n < (4095-1)/2$ and $\Delta v = 300/2094$ mv. Any value above +300 mv or below -300 mv was assigned the value of +300 mv or -300 mv respectively, i.e., the upper limitation was 600 mv p-p. It can also be seen that the range of values should be spread as much as possible over the 600 mv limit. Otherwise, the number of groups would be small and an effective distribution analysis impossible.

After arranging the samples into groups, the program provided a histogram and a cumulative distribution function. An example of the output for one run is shown in Figs. (4.3) and (4.4).

## Results

The computer results for the distribution functions were plotted on normal distribution graph paper, examples of which are given in Figs. (4.5) through (4.21). A representative selection of samples has been included for the range of C/N ratios studied. Graphs containing useful information have been included.

It can be seen that a significant departure from a normal distribution occurs at a C/N ratio of 10 dB. Consider Fig. (4.9) representing a C/N ratio of 10 dB and a baseband slot at 70 KHz. About 2 percent of the samples have a significantly higher magnitude than predicted by a normal distribution (a 2 percent figure represents about 400 samples). The graphs for 105 KHz and 290 KHz slots show a similar deviation from a normal distribution, cf., Figs. (4.10) and (4.11) respectively. The other C/N ratios show no significant deviation, except for values below the .05 percent point or above the 99.95 percent point. It must be noted, however, that these constitute less than 0.1 percent of the total, or about 10-20 samples. Hence a significant effect is produced by each sample, and no reliable information can be deduced from them.

The following table illustrates the significance of Fig. (4.9).

Table 4.1 - Comparison of Gaussian distribution with the probability distribution at threshold.

| x(mv) | P(X < x) Gaussian | P(X < x) Actual |
|---|---|---|
| -65 | .031 | .033 |
| -85 | .0065 | .009 |
| -105 | .001 | .0035 |
| -125 | <.0001 | .0008 |

The occurrence of a non-Gaussian distribution in the threshold region has been expected. As mentioned previously, the discriminator output will be non-Gaussian over most of the range studied. It is the use of the low-pass output filter which generally causes the Gaussian form of the output (central limit theorem). However, when the average click rate is appreciably greater than 1/T, where T is the time of the run (about 2-3 seconds), but less than $f_m$ where $f_m$ is the output filter cutoff frequency, the individual nature of the "clicks" will become apparent. The output will then have a non-Gaussian distribution.

It has been shown that a 2 dB decrease in the C/N ratio near threshold can increase the click rate by a factor approaching 100.[11] The non-Gaussian output will then occur for a relatively small range of C/N ratios, as indicated by the experimental data.

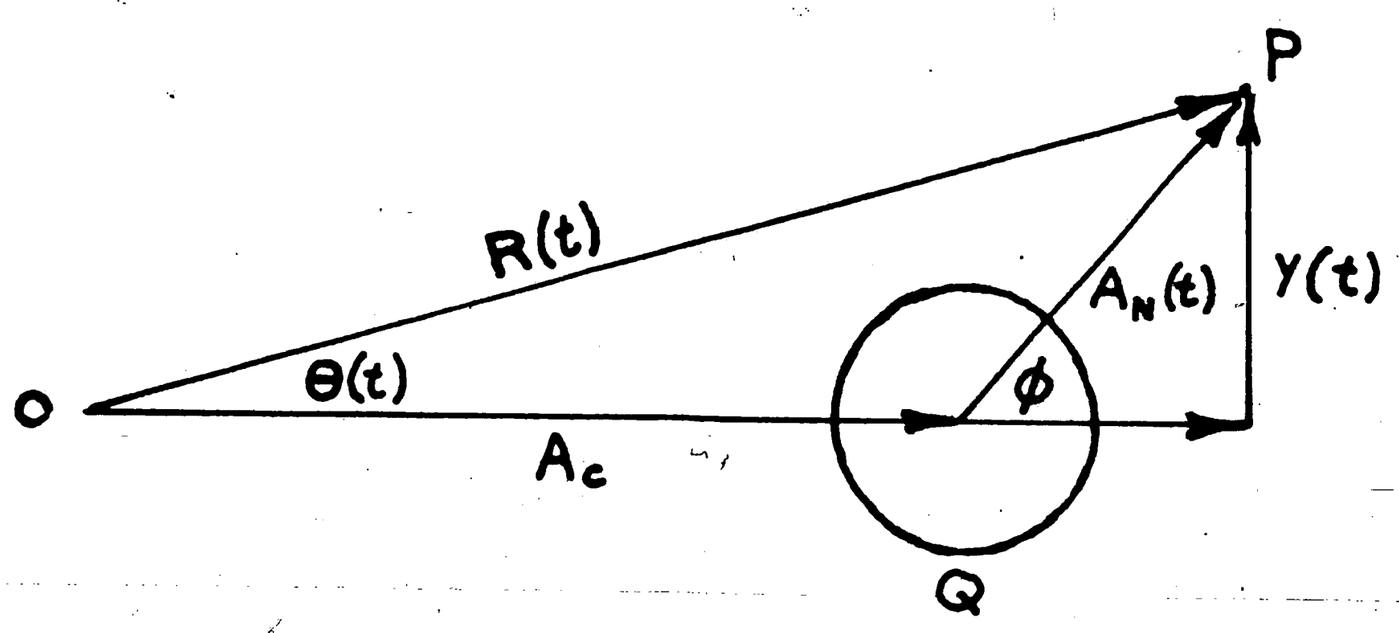


Fig. 3.1 - Phasor representation of noise plus carrier.

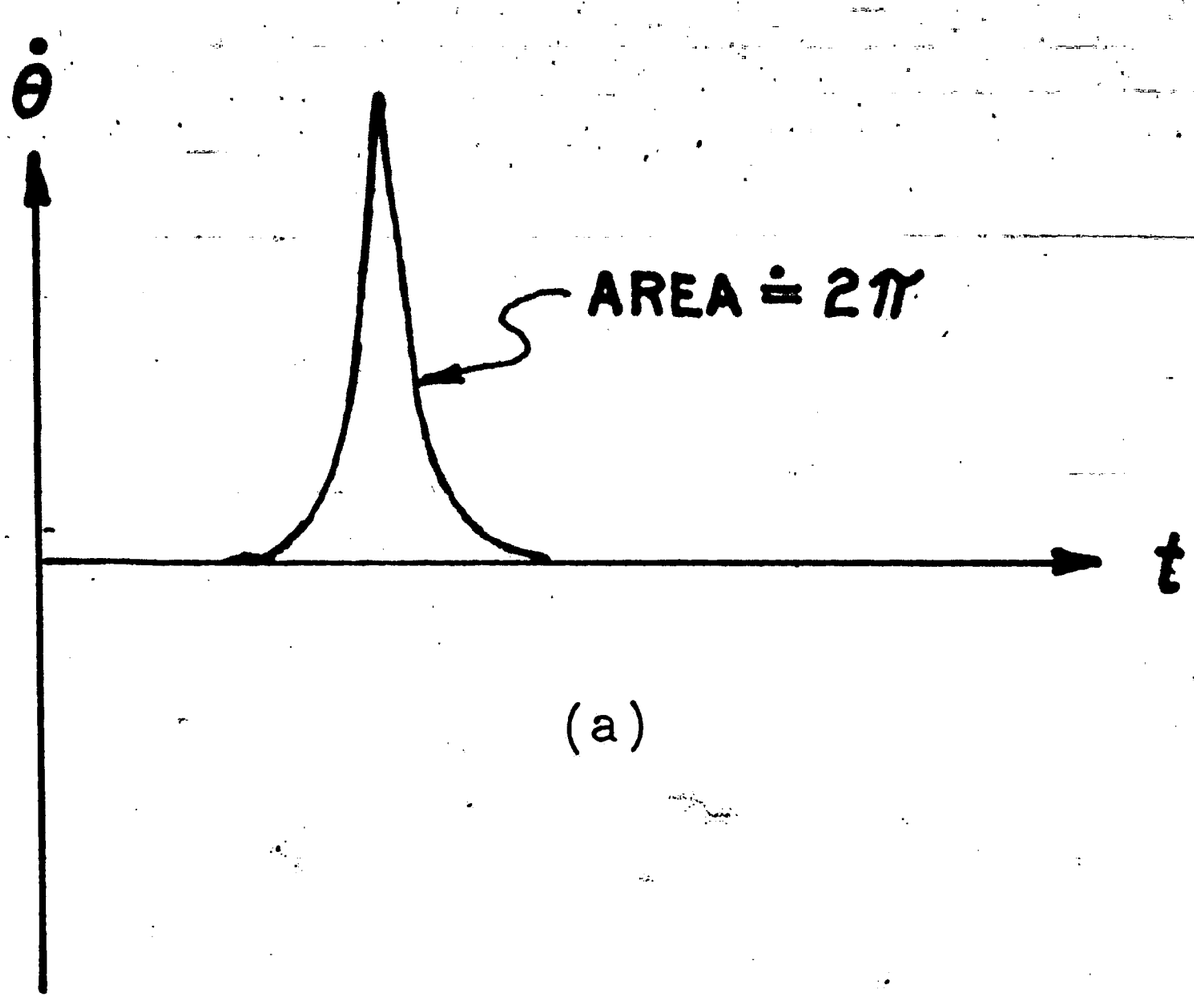


Fig. 3.2 - Click and non-click producing discriminator pulses.

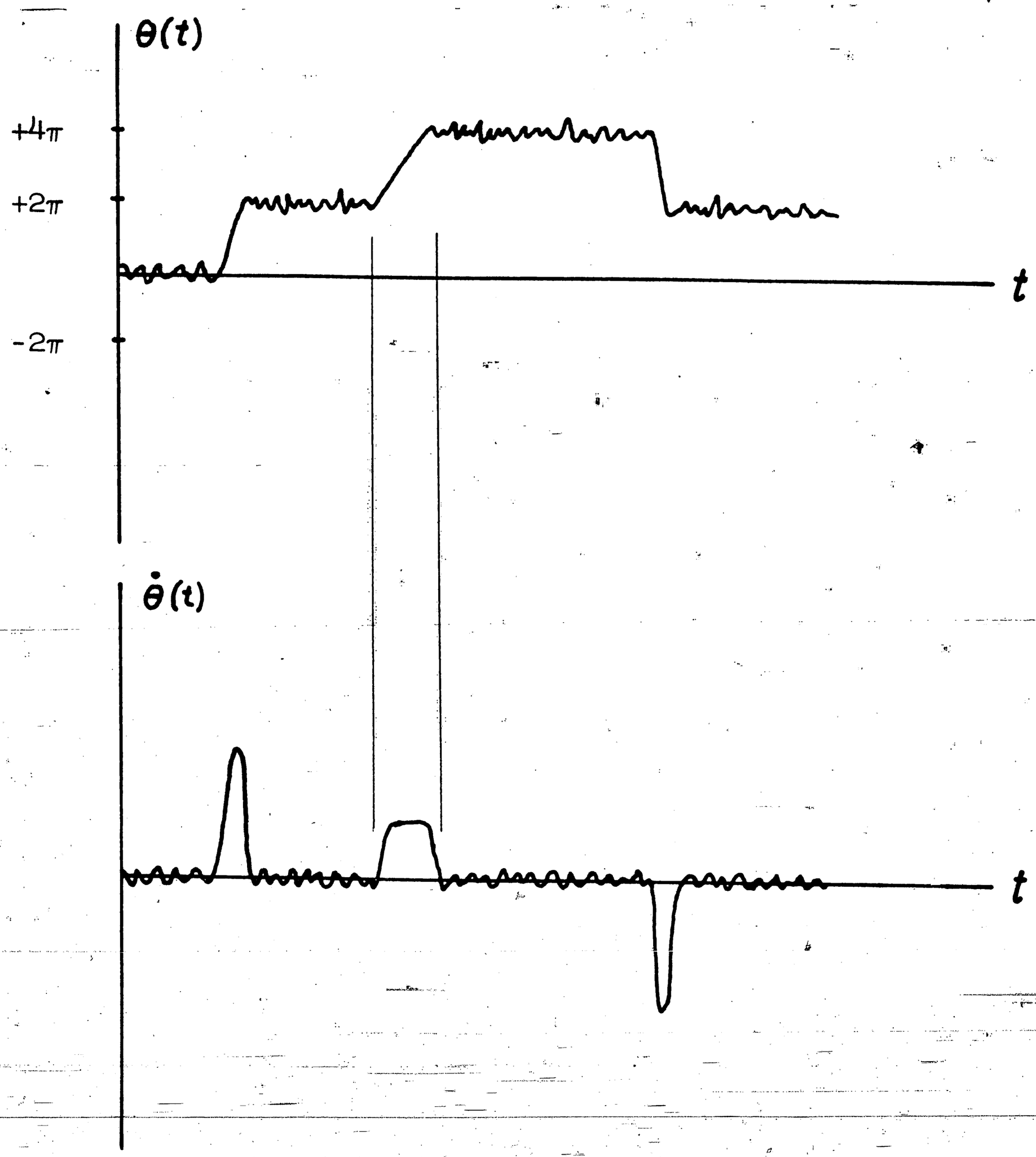


Fig. 3.3 - Phase angle changes and their effects on discriminator output.

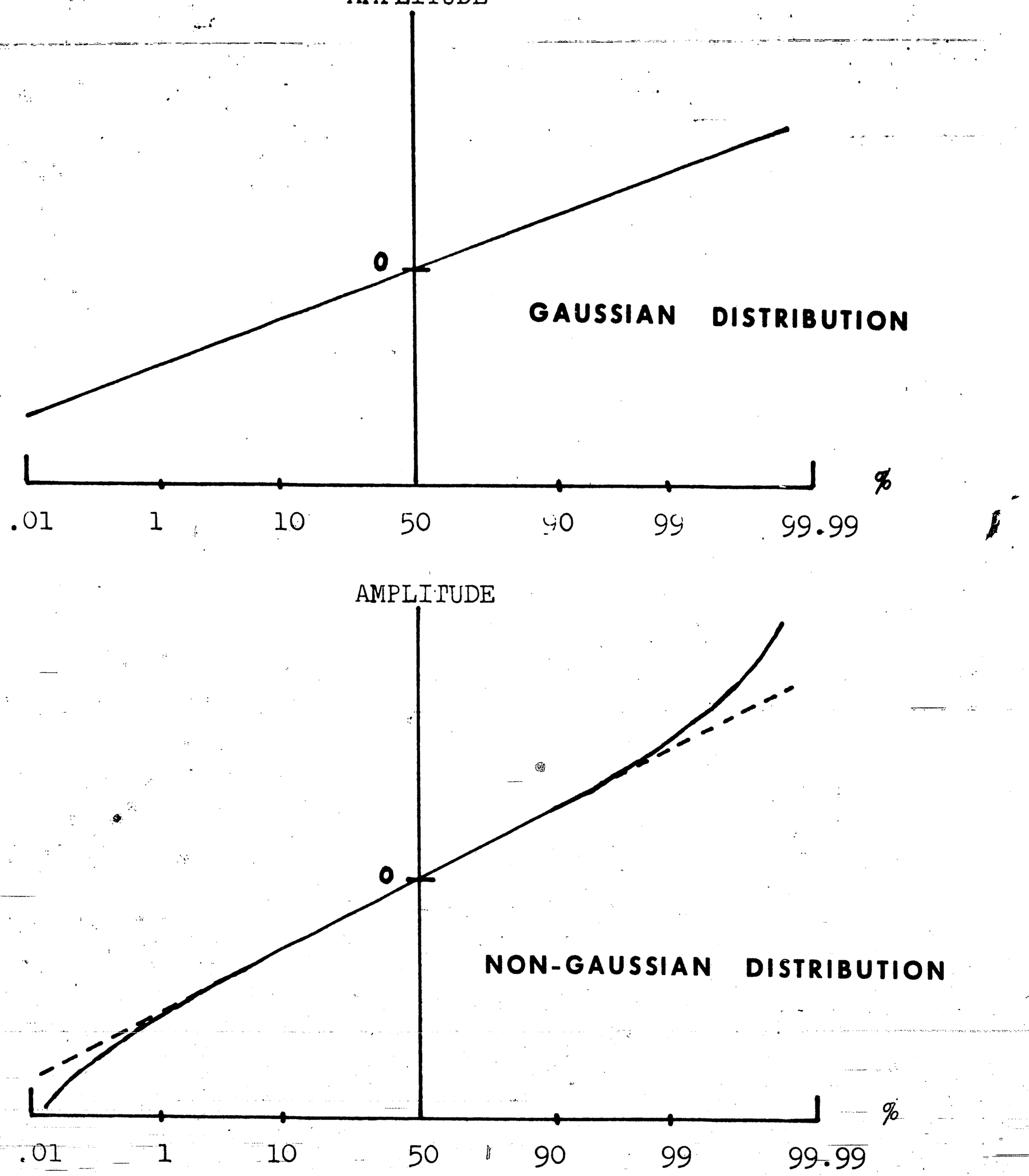


Fig. 3.4 - Noise distribution at filter output.

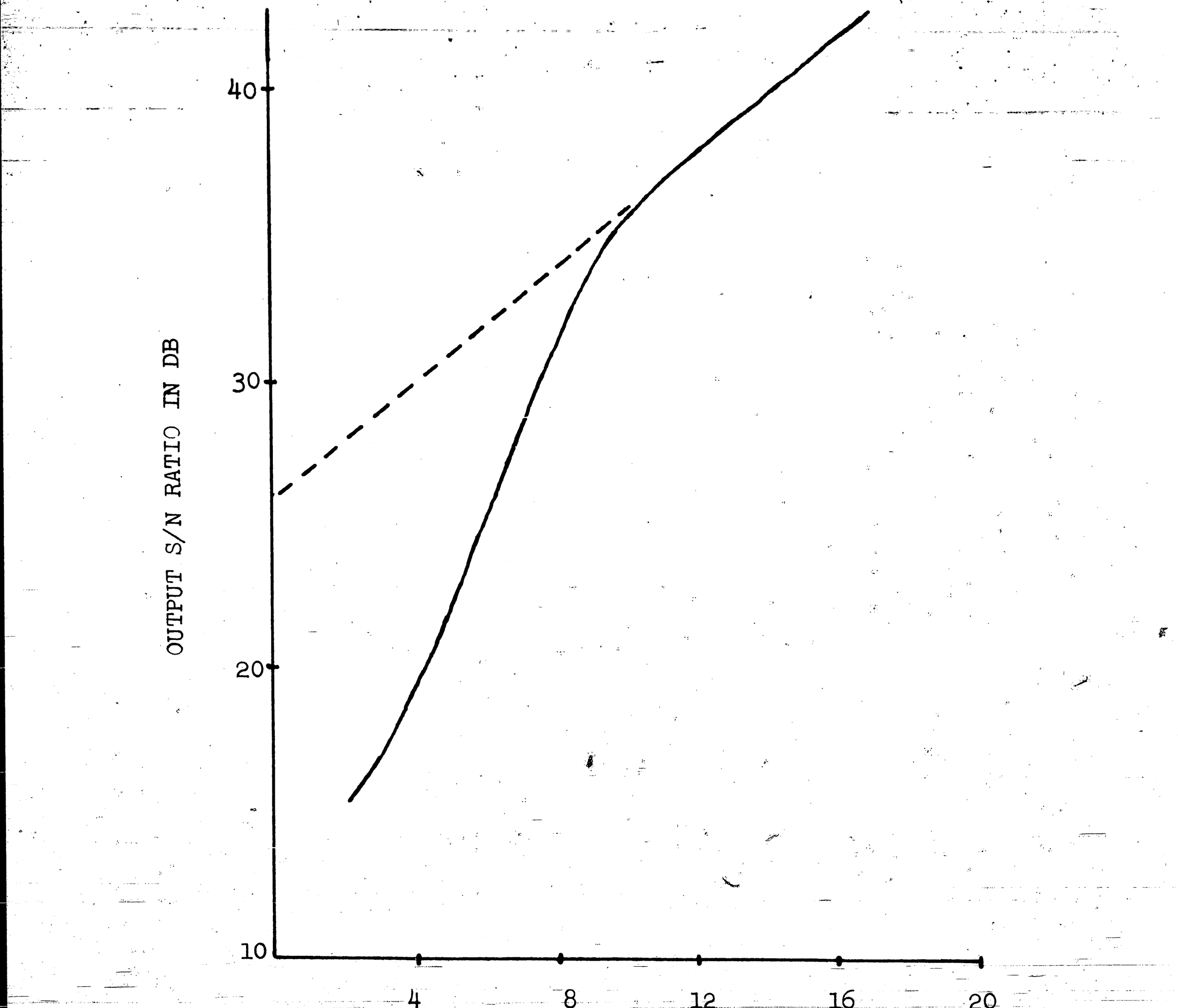


Fig. 3.5 - Signal-to-noise ratio vs. carrier-to-noise ratio.

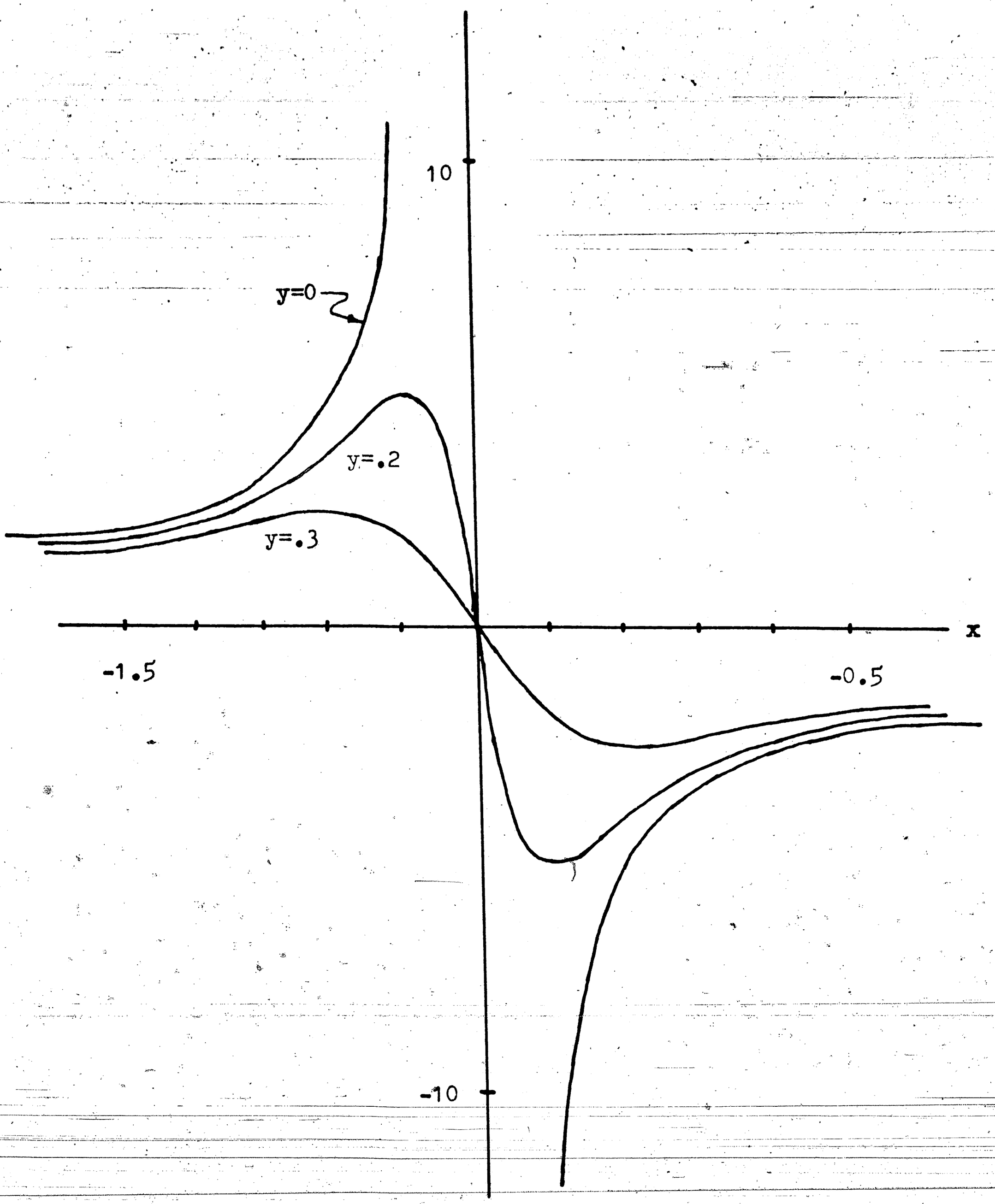


Fig. 3.6 - Behavior of discriminator output coefficient P(t) (with A=1).

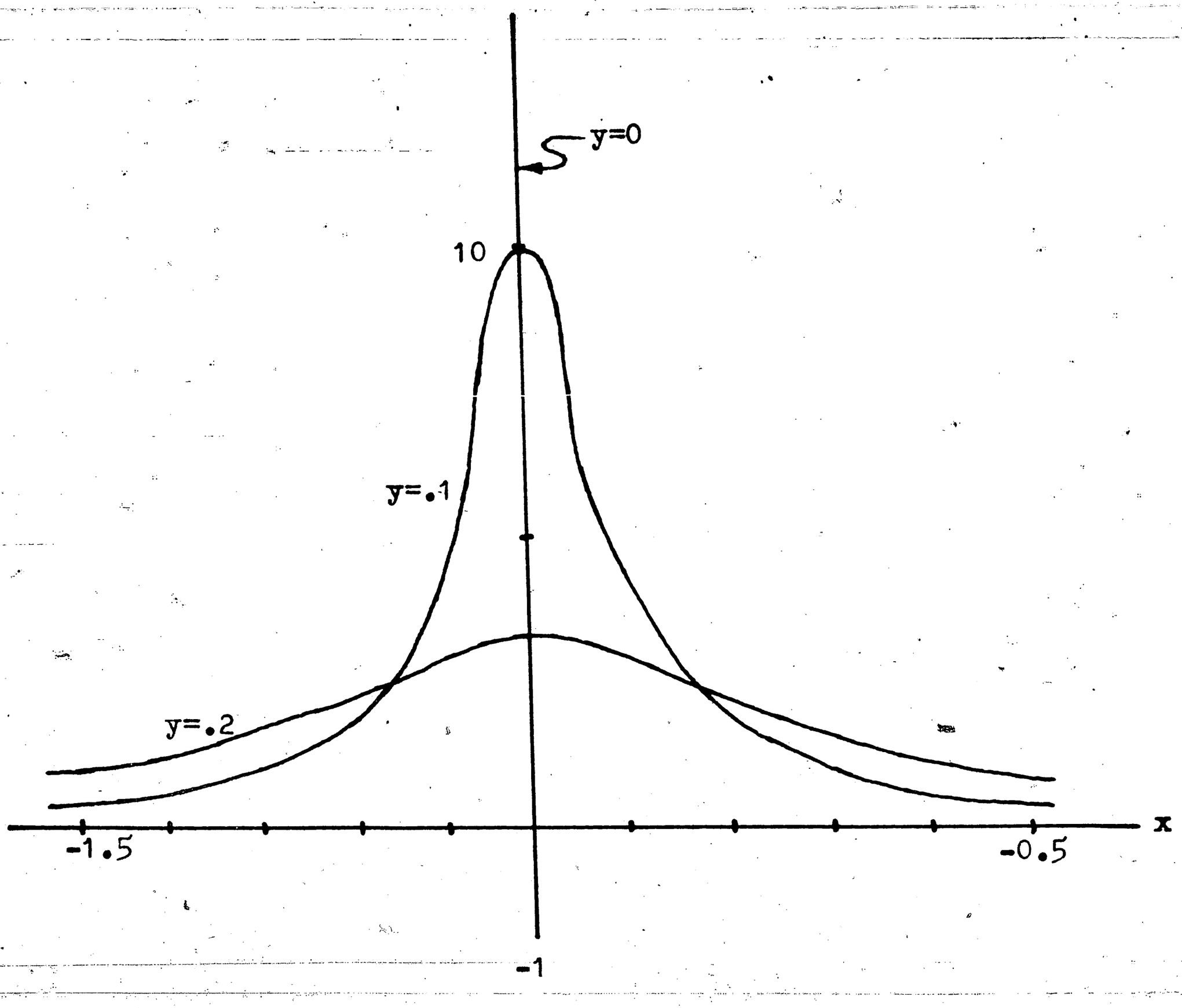


Fig. 3.7 - Behavior of discriminator output coefficient S(t) (with A=1).

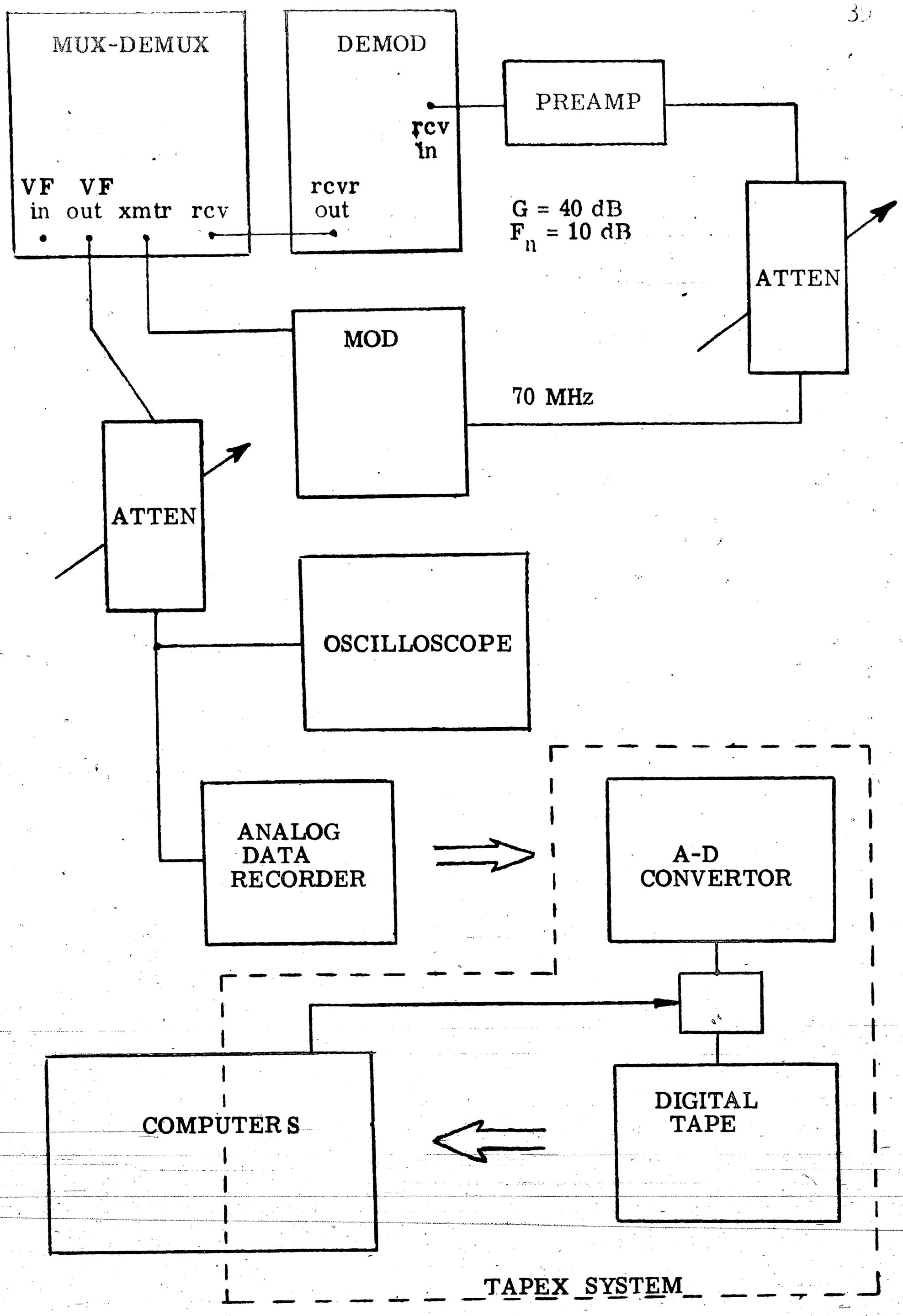


Fig. 4.1 - Block diagram of the experimental set-up.

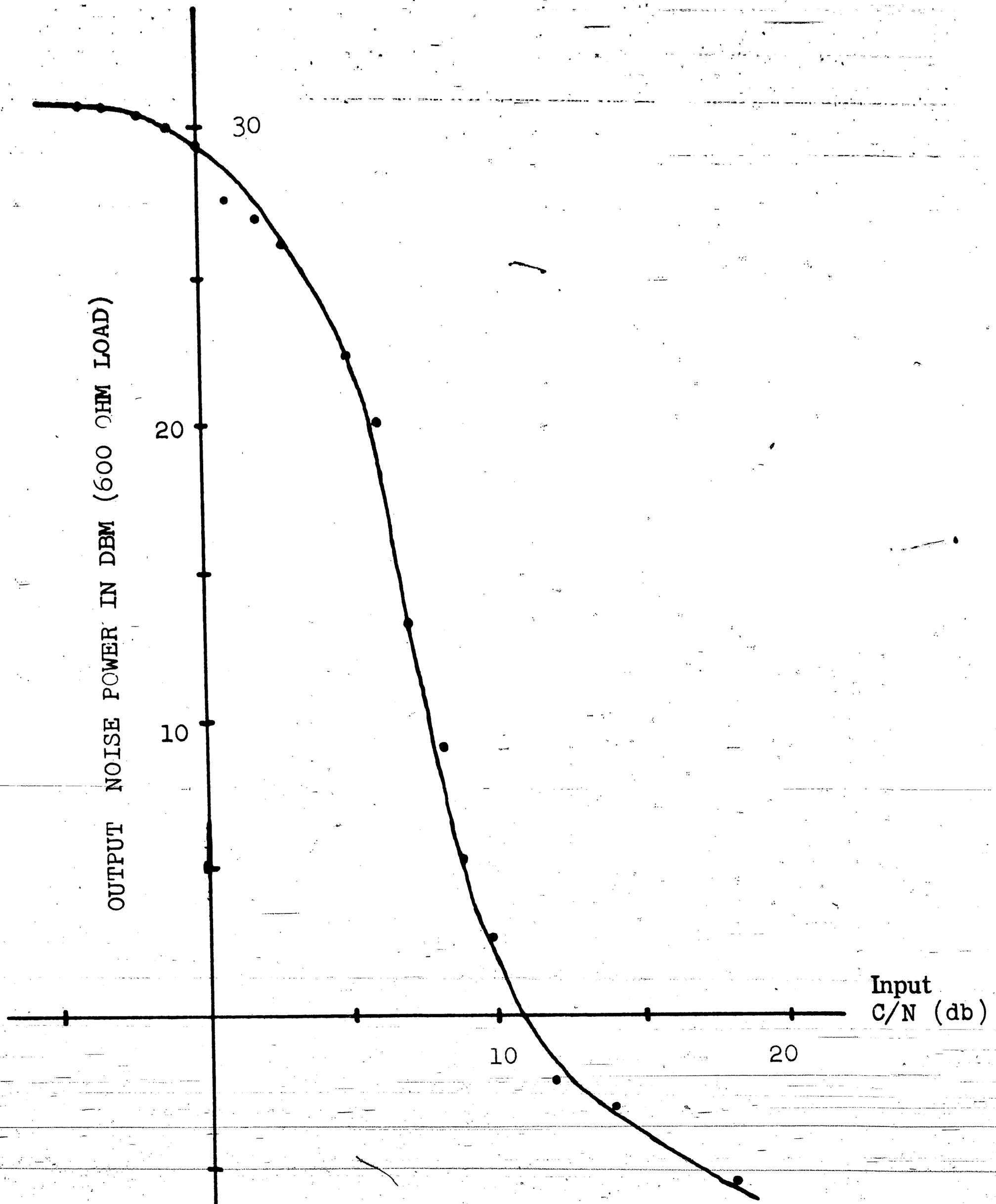


Fig. 4.2 - Noise output dependence on carrier-to-noise ratio.

HISTØGRAM ØF NØISE DISTRIBUTIØN

| MVØLTS | SAMPLES |
|---|---|
| -295.0 | C. |
| -285.0 | C. |
| -275.0 | C. |
| -265.0 | C. |
| -255.0 | C. |
| -245.0 | C. |
| -235.0 | C. |
| -225.0 | C. |
| -215.0 | C. |
| -205.0 | 1. |
| -195.0 | 1. |
| -185.0 | 1. |
| -175.0 | C. |
| -165.0 | 1. |
| -155.0 | 4. |
| -145.0 | 4. |
| -135.0 | 3. |
| -125.0 | 7. |
| -115.0 | 14. |
| -105.0 | 15. |
| -95.0 | 27. |
| -85.0 | 56. |
| -75.0 | 115. |
| -65.0 | 263. |
| -55.0 | 423. |
| -45.0 | 668. |
| -35.0 | 1068. |
| -25.0 | 1426. |
| -15.0 | 1568. |
| -5.0 | 1892. |
| 5.0 | 1830. |
| 15.0 | 1653. |
| 25.0 | 1305. |
| 35.0 | 1033. |
| 45.0 | 798. |
| 55.0 | 400. |
| 65.0 | 242. |
| 75.0 | 127. |
| 85.0 | 67. |
| 95.0 | 42. |
| 105.0 | 11. |
| 115.0 | 8. |
| 125.0 | 3. |
| 135.0 | 2. |
| 145.0 | 2. |
| 155.0 | 1. |
| 165.0 | 2. |
| 175.0 | 1. |
| 185.0 | 3. |
| 195.0 | C. |
| 205.0 | 1. |
| 215.0 | 1. |
| 225.0 | C. |
| 235.0 | C. |
| 245.0 | C. |
| 255.0 | C. |
| 265.0 | C. |
| 275.0 | C. |
| 285.0 | 1. |
| 295.0 | C. |

Fig. 4.3 - Histogram of noise distribution with C/N = 10 dB and the band slot at 70 kHz.

CUMULATIVE DISTRIBUTION OF NOISE

| MVOLTS | CUM |
|---|---|
| -295.0 | 0. |
| -285.0 | 0. |
| -275.0 | 0. |
| -265.0 | 0. |
| -255.0 | 0. |
| -245.0 | 0. |
| -235.0 | 0. |
| -225.0 | 0. |
| -215.0 | 0. |
| -205.0 | 0.00006653 |
| -195.0 | 0.00013307 |
| -185.0 | 0.00019960 |
| -175.0 | 0.00019960 |
| -165.0 | 0.00026613 |
| -155.0 | 0.00053227 |
| -145.0 | 0.00079840 |
| -135.0 | 0.00099800 |
| -125.0 | 0.00146374 |
| -115.0 | 0.00239521 |
| -105.0 | 0.00339321 |
| -95.0 | 0.00518962 |
| -85.0 | 0.00891550 |
| -75.0 | 0.01656687 |
| -65.0 | 0.03406520 |
| -55.0 | 0.06220891 |
| -45.0 | 0.10665336 |
| -35.0 | 0.17371523 |
| -25.0 | 0.26859614 |
| -15.0 | 0.37292082 |
| -5.0 | 0.49880239 |
| 5.0 | 0.62055887 |
| 15.0 | 0.73053891 |
| 25.0 | 0.81736526 |
| 35.0 | 0.88609447 |
| 45.0 | 0.93918827 |
| 55.0 | 0.96580171 |
| 65.0 | 0.98190284 |
| 75.0 | 0.99035260 |
| 85.0 | 0.99481035 |
| 95.0 | 0.99760476 |
| 105.0 | 0.99833662 |
| 115.0 | 0.99886868 |
| 125.0 | 0.99906848 |
| 135.0 | 0.99920154 |
| 145.0 | 0.99933460 |
| 155.0 | 0.99940112 |
| 165.0 | 0.99953418 |
| 175.0 | 0.99960071 |
| 185.0 | 0.99980030 |
| 195.0 | 0.99980030 |
| 205.0 | 0.99986683 |
| 215.0 | 0.99993335 |
| 225.0 | 0.99993335 |
| 235.0 | 0.99993335 |
| 245.0 | 0.99993335 |
| 255.0 | 0.99993335 |
| 265.0 | 0.99993335 |
| 275.0 | 0.99993335 |
| 285.0 | 0.99999918 |
| 295.0 | 0.99999918 |

MEAN IS 0.25349
SIGMA IS 33.68910

Fig. 4.4 - Cumulative distribution of noise with C/N = 10 dB and the band slot at 70 kHz.

## NOISE DISTRIBUTION

C/N = 14 dB

Band Slot at 70 KHz

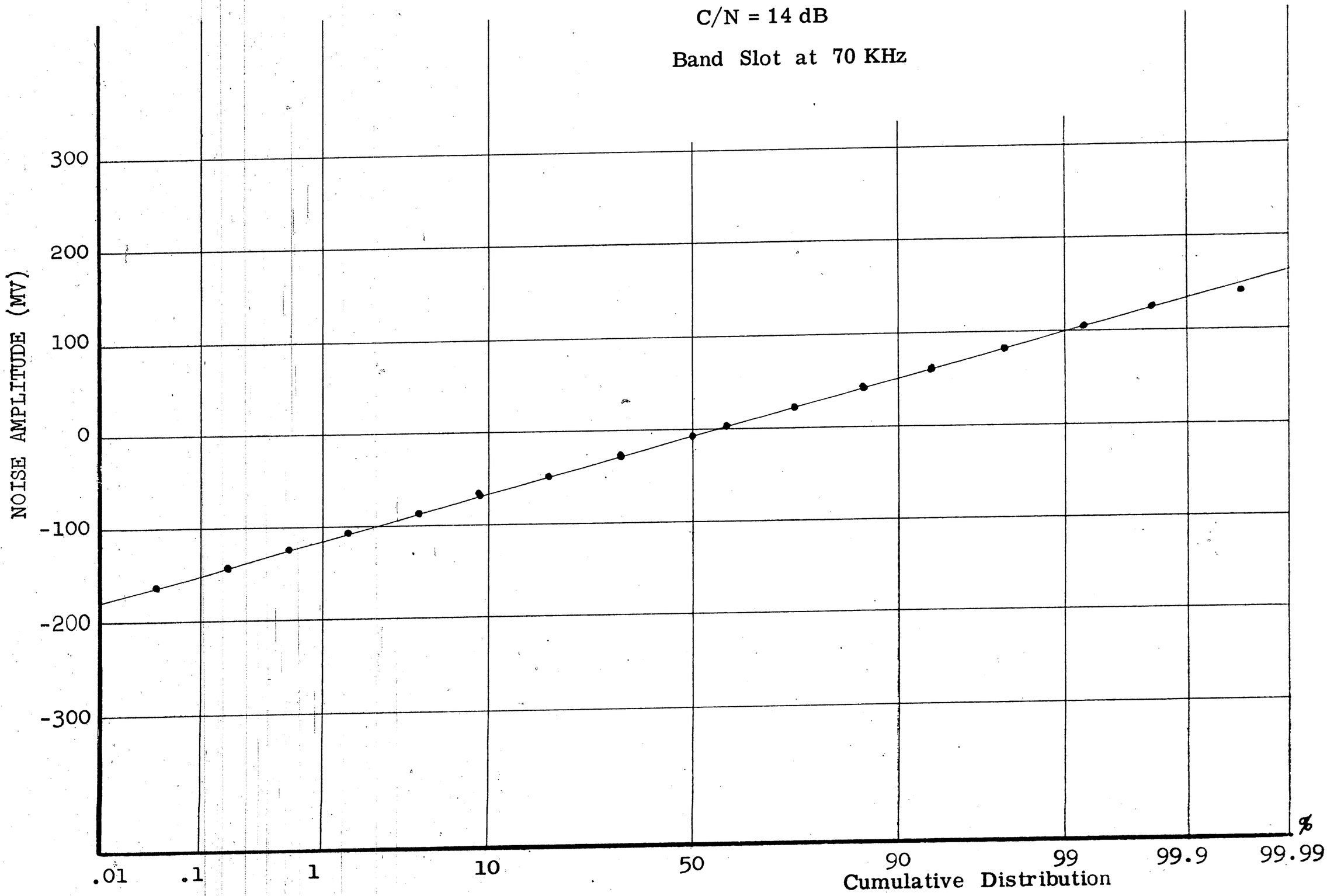


Figure 4.5

## NOISE DISTRIBUTION

C/N = 14 dB

Band Slot at 105 KHz

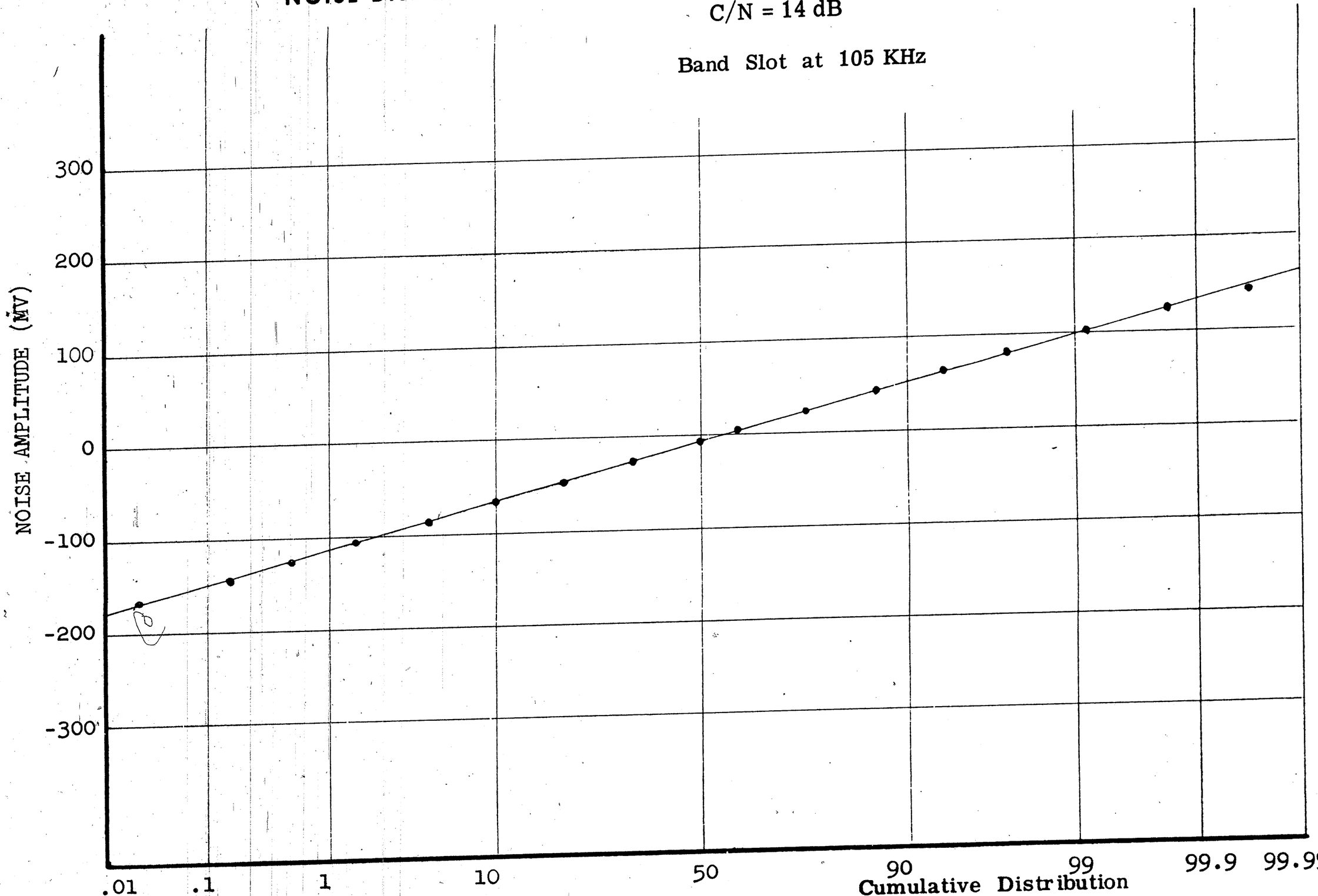


Figure 4.6

**NOISE DISTRIBUTION**

C/N = 14 dB

Band Slot at 290 KHz

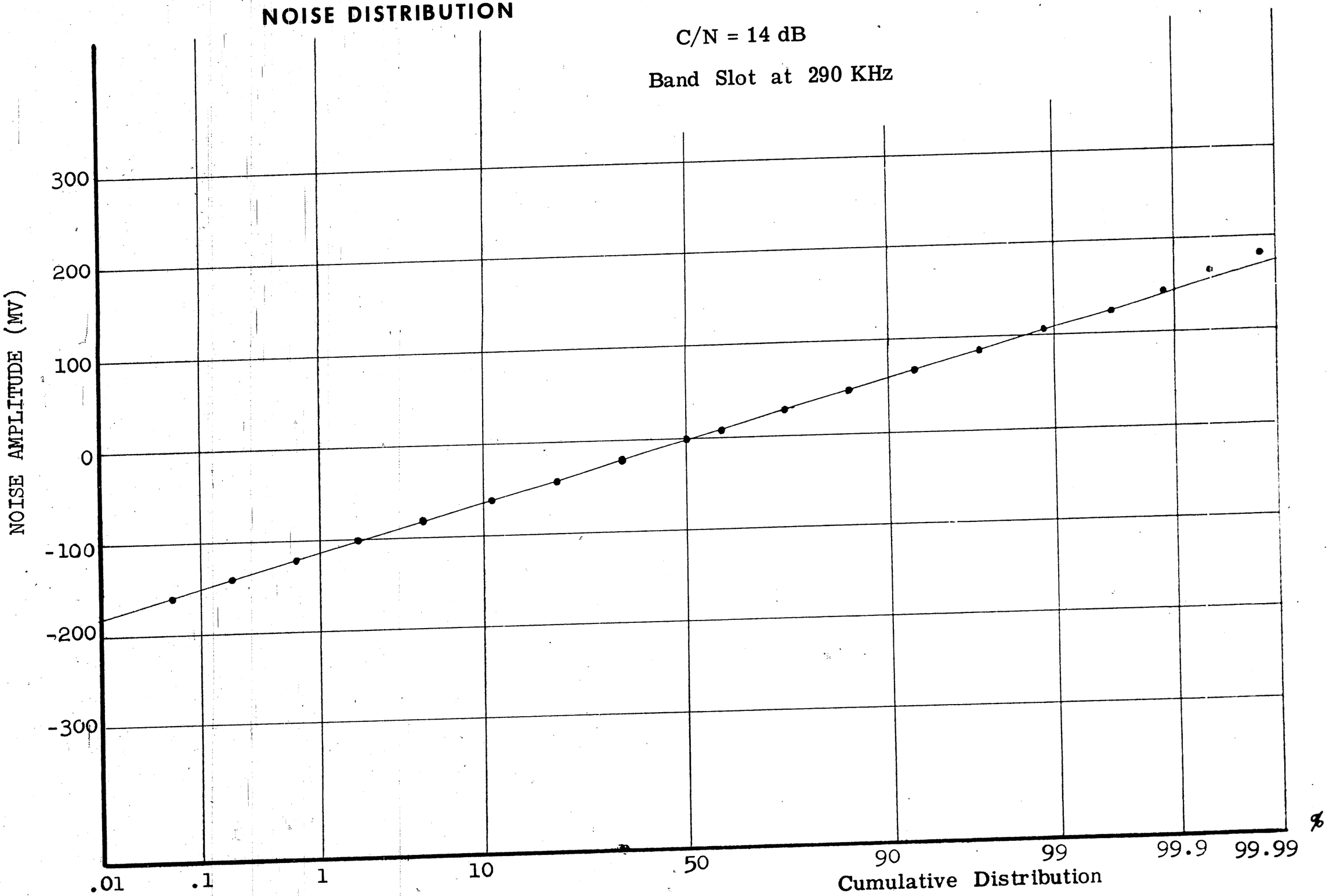


Figure 4.7

## NOISE DISTRIBUTION

C/N = 12 dB

Band Slot at 70 KHz

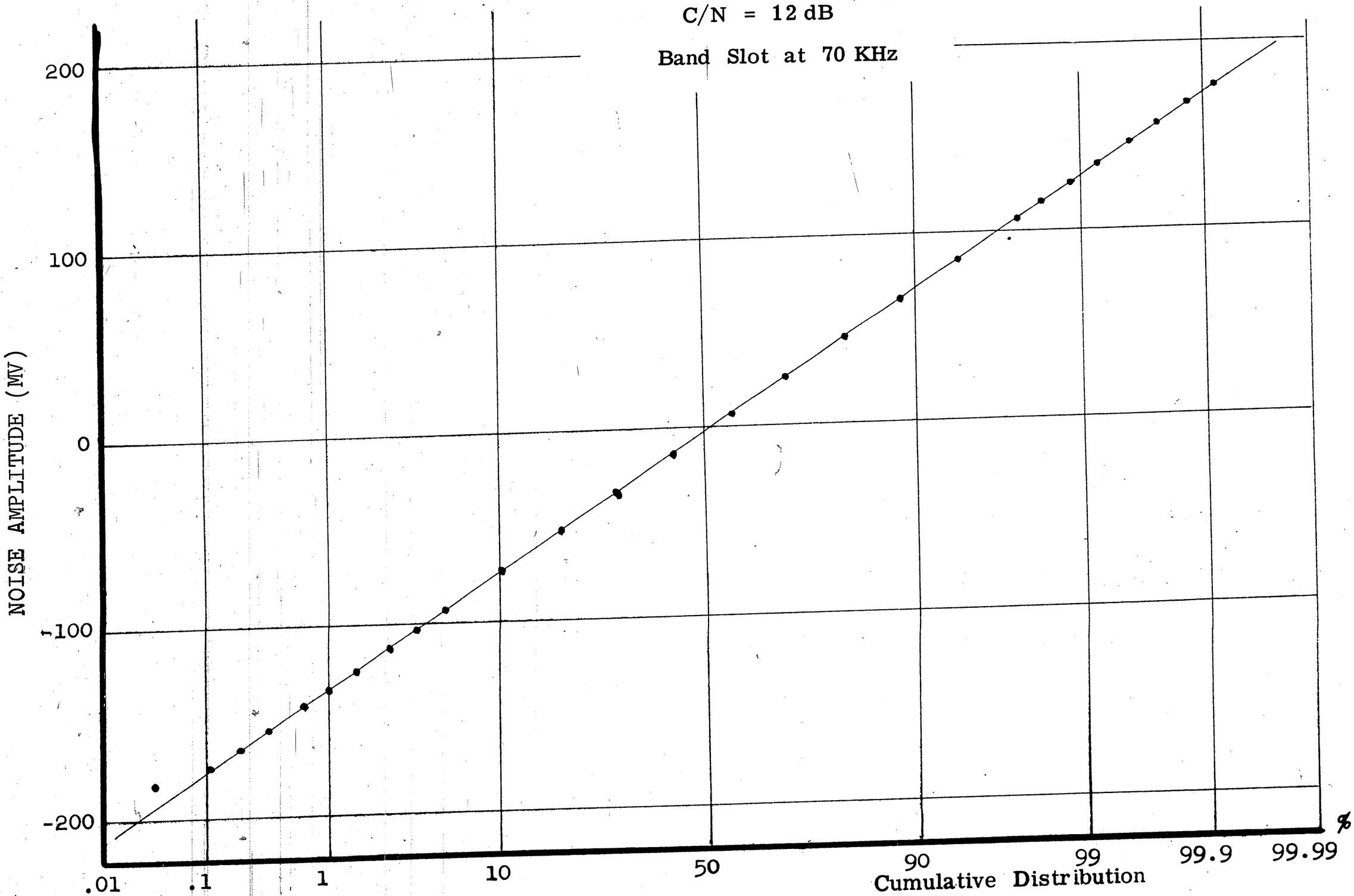


Figure 4.8

## NOISE DISTRIBUTION

C/N = 10 dB

Band Slot at 70 KHz

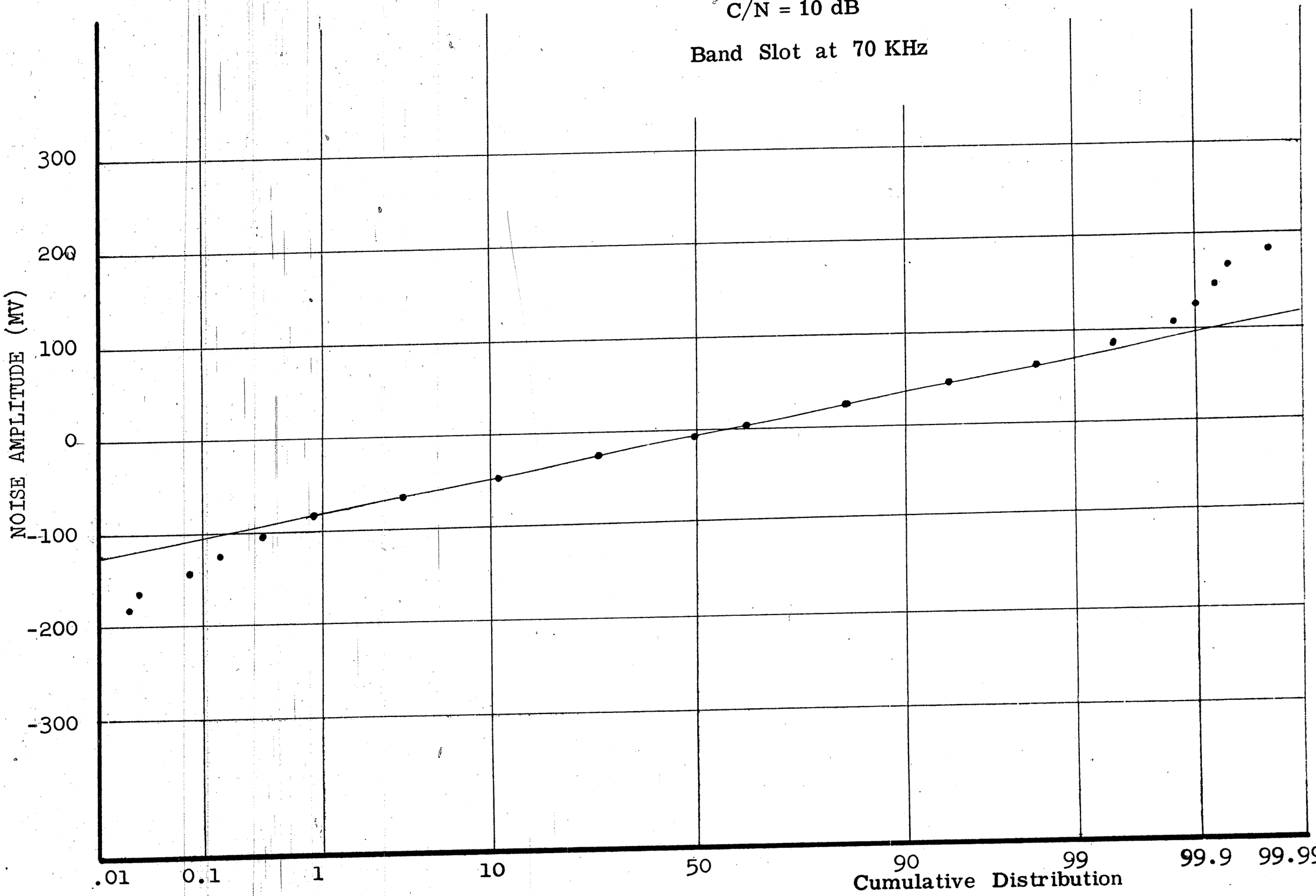


Figure 4.9

## NOISE DISTRIBUTION

C/N = 10 dB

Band Slot at 105 KHz

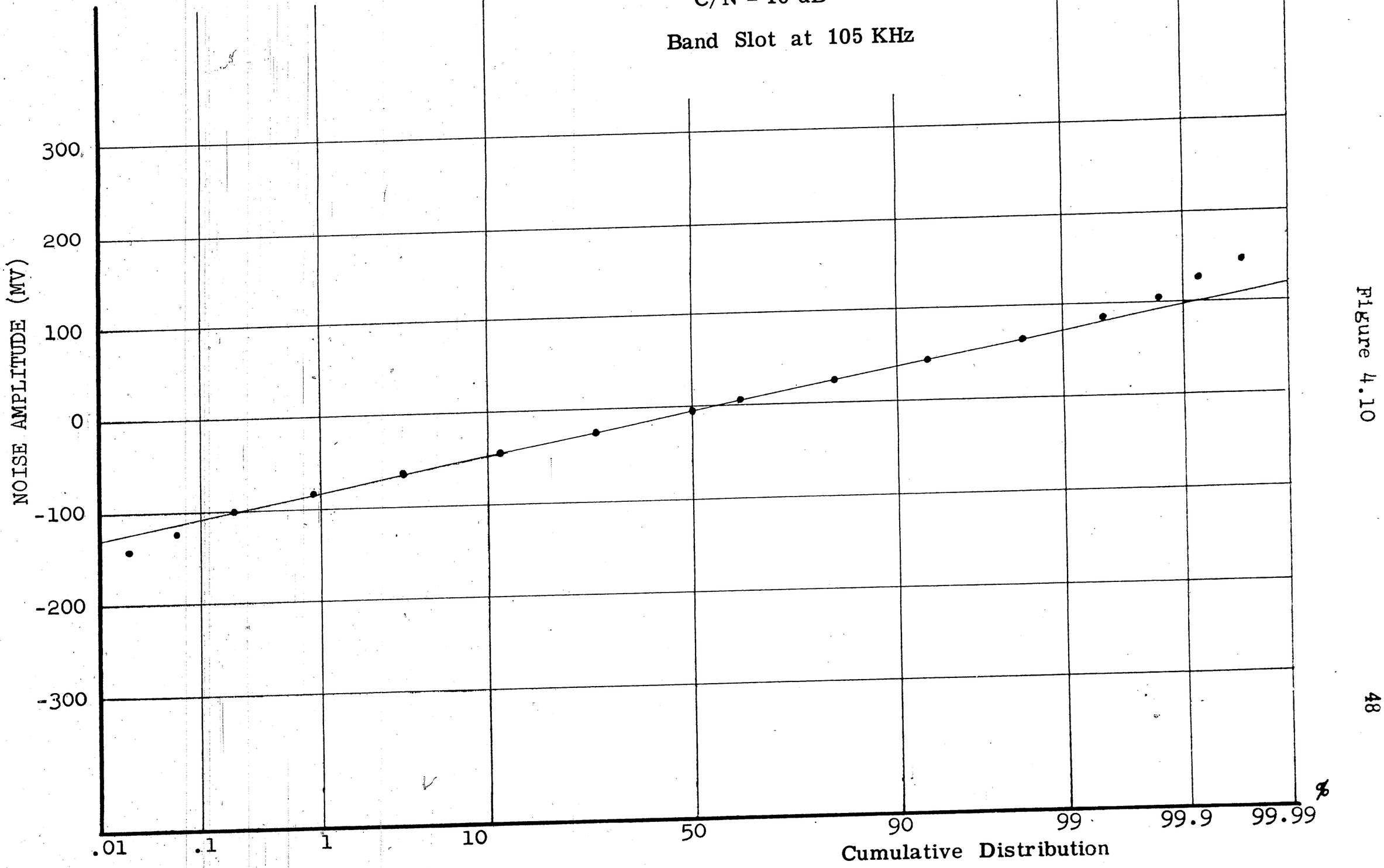


Figure 4.10

## NOISE DISTRIBUTION

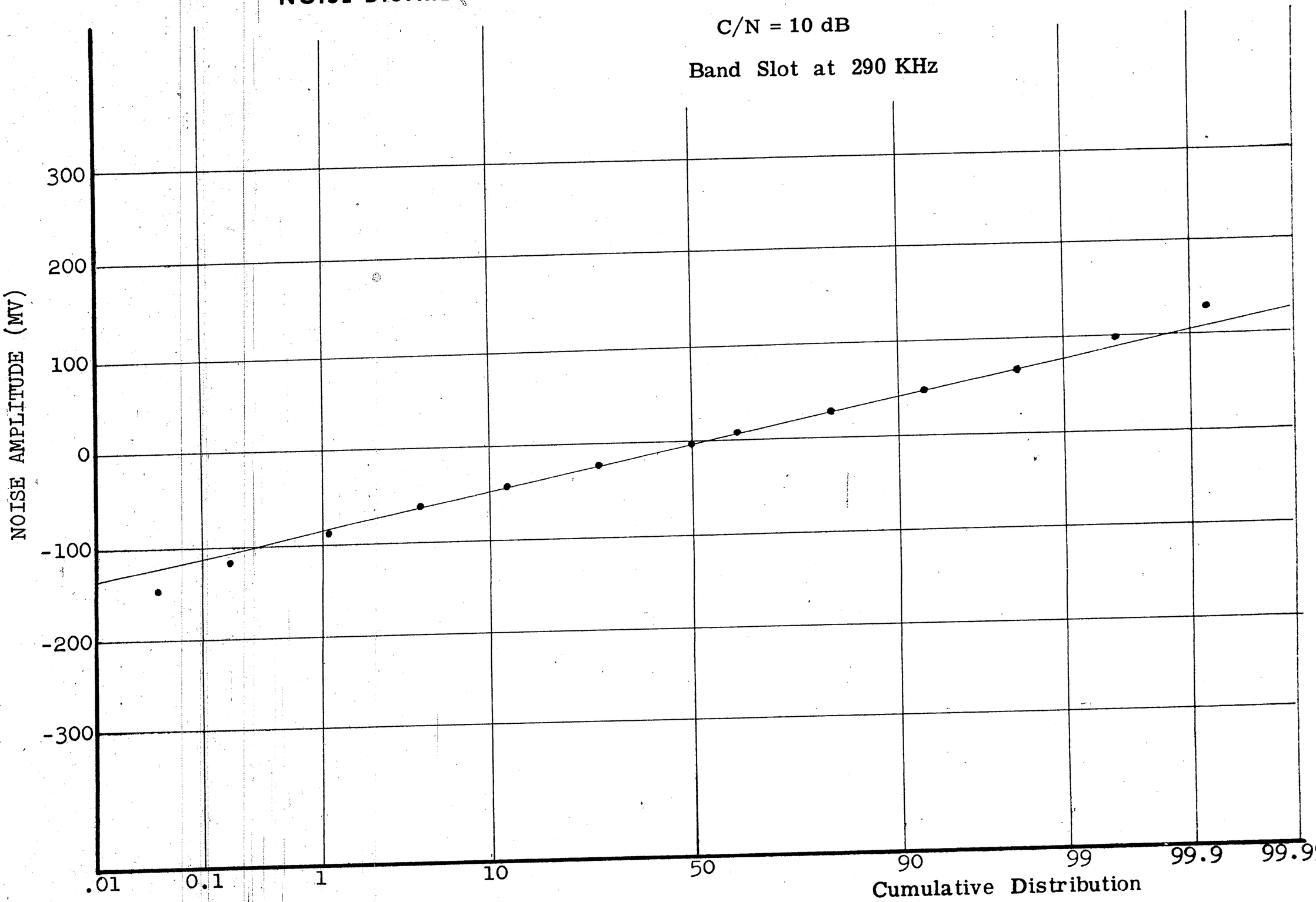


Figure 4.11

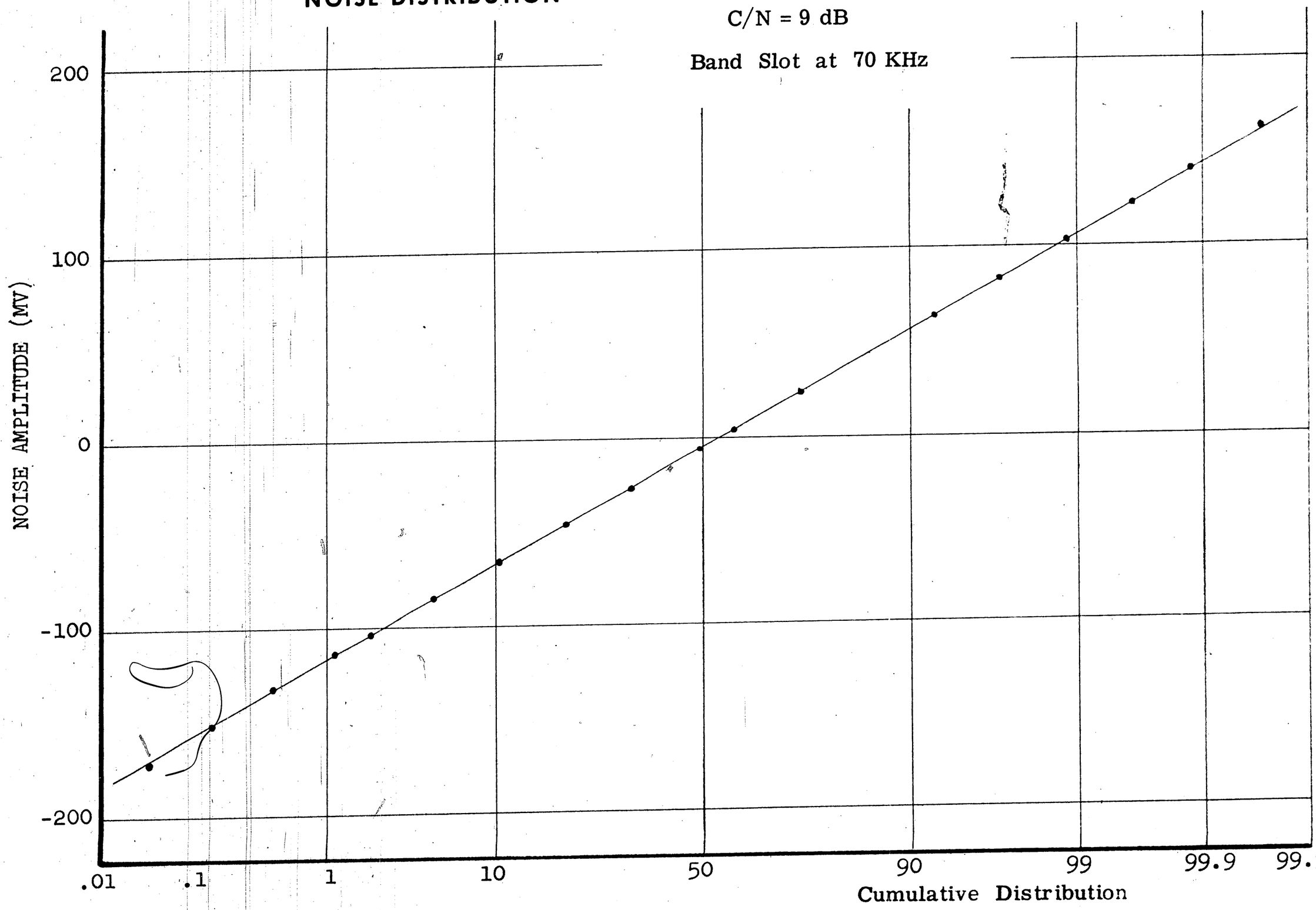
NOISE DISTRIBUTION
C/N = 9 dB
Band Slot at 70 KHz
NOISE AMPLITUDE (MV)
200
100
0
-100
-200
.01
.1
1
10
50
90
99
99.9
99.99
%
Cumulative Distribution

Figure 4.12

## NOISE DISTRIBUTION

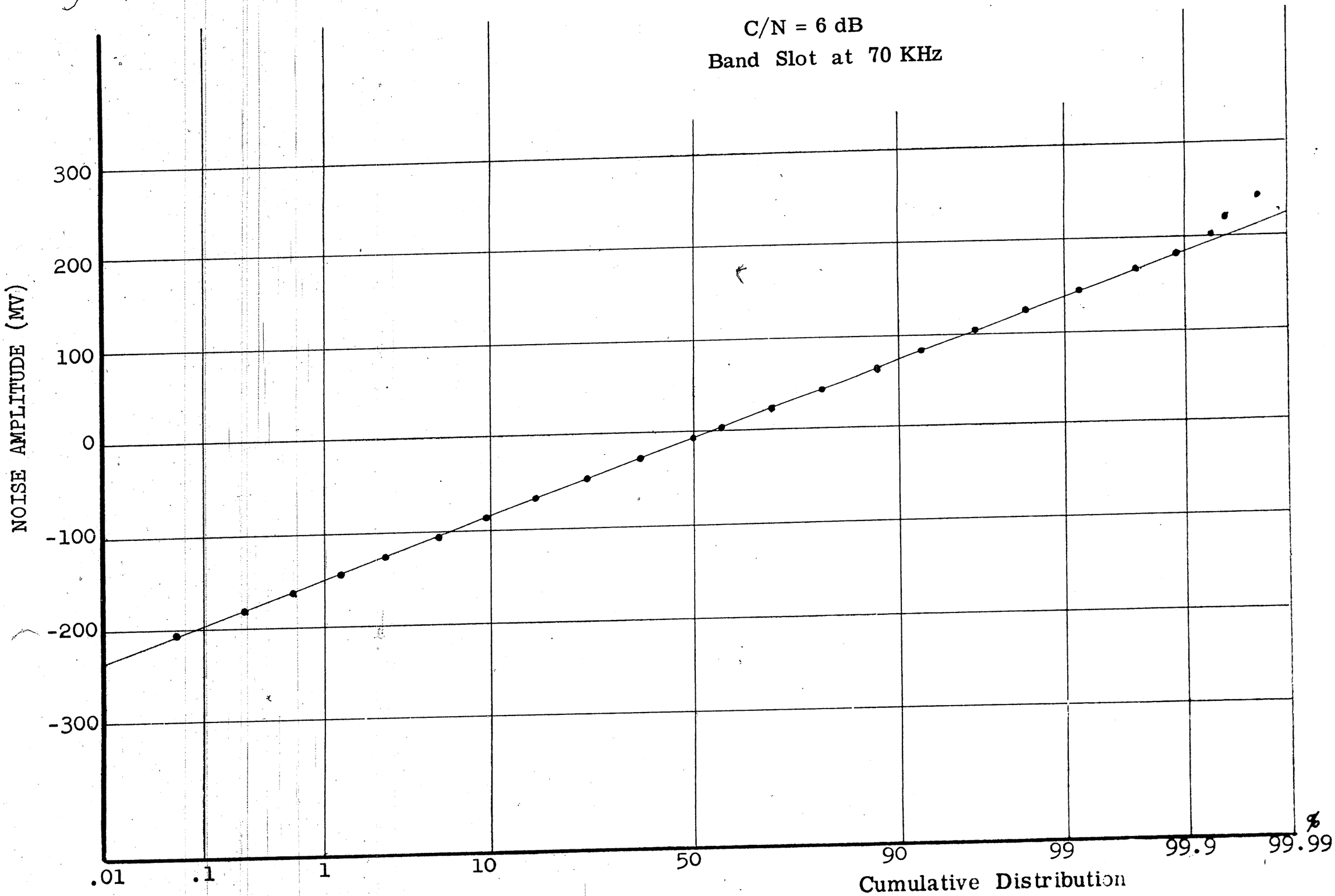


Figure 4.13

## NOISE DISTRIBUTION

C/N = 6 dB

Band Slot at 105 KHz

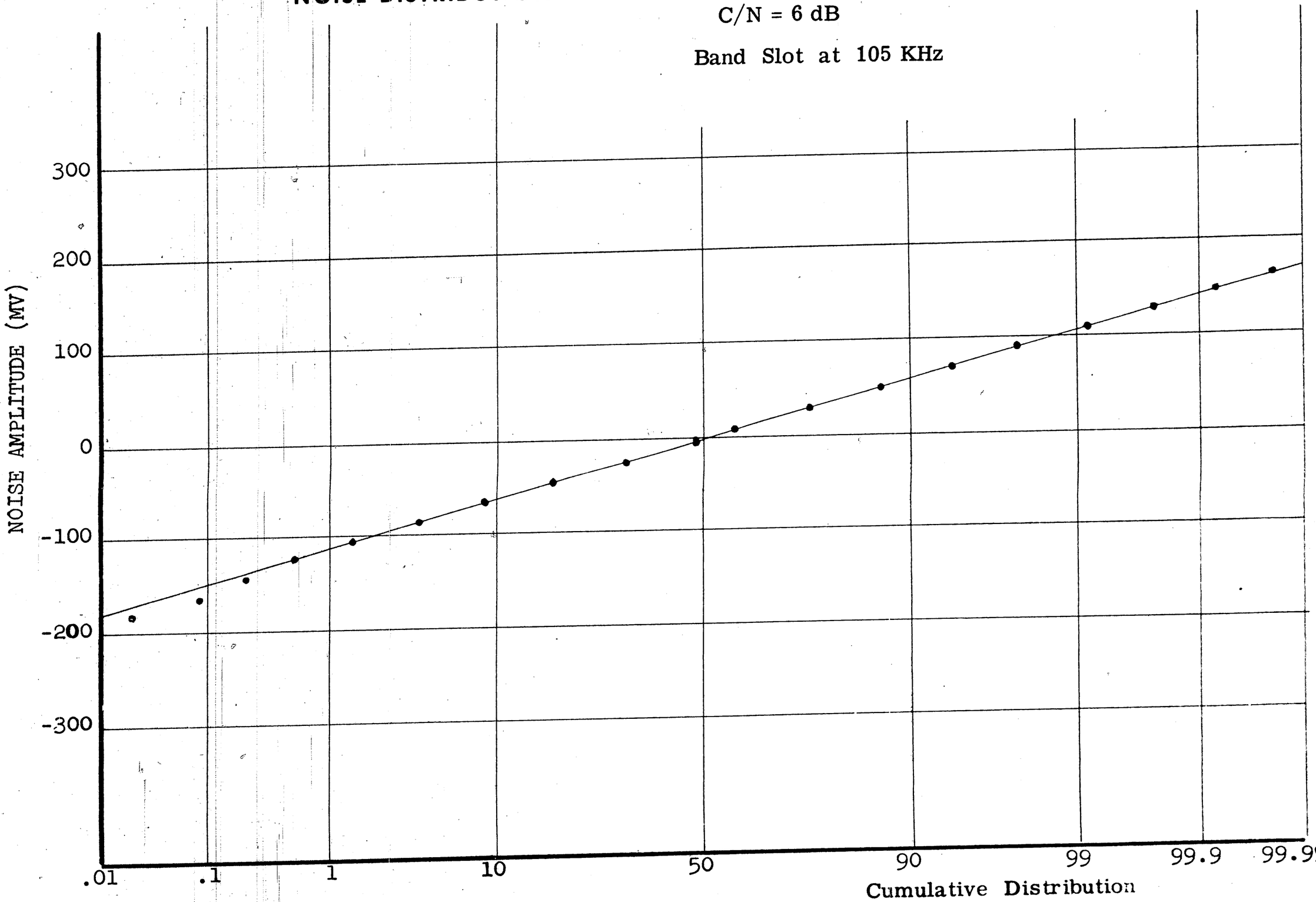


Figure 4.14

## NOISE DISTRIBUTION

C/N = 6 dB

Band Slot at 290 KHz

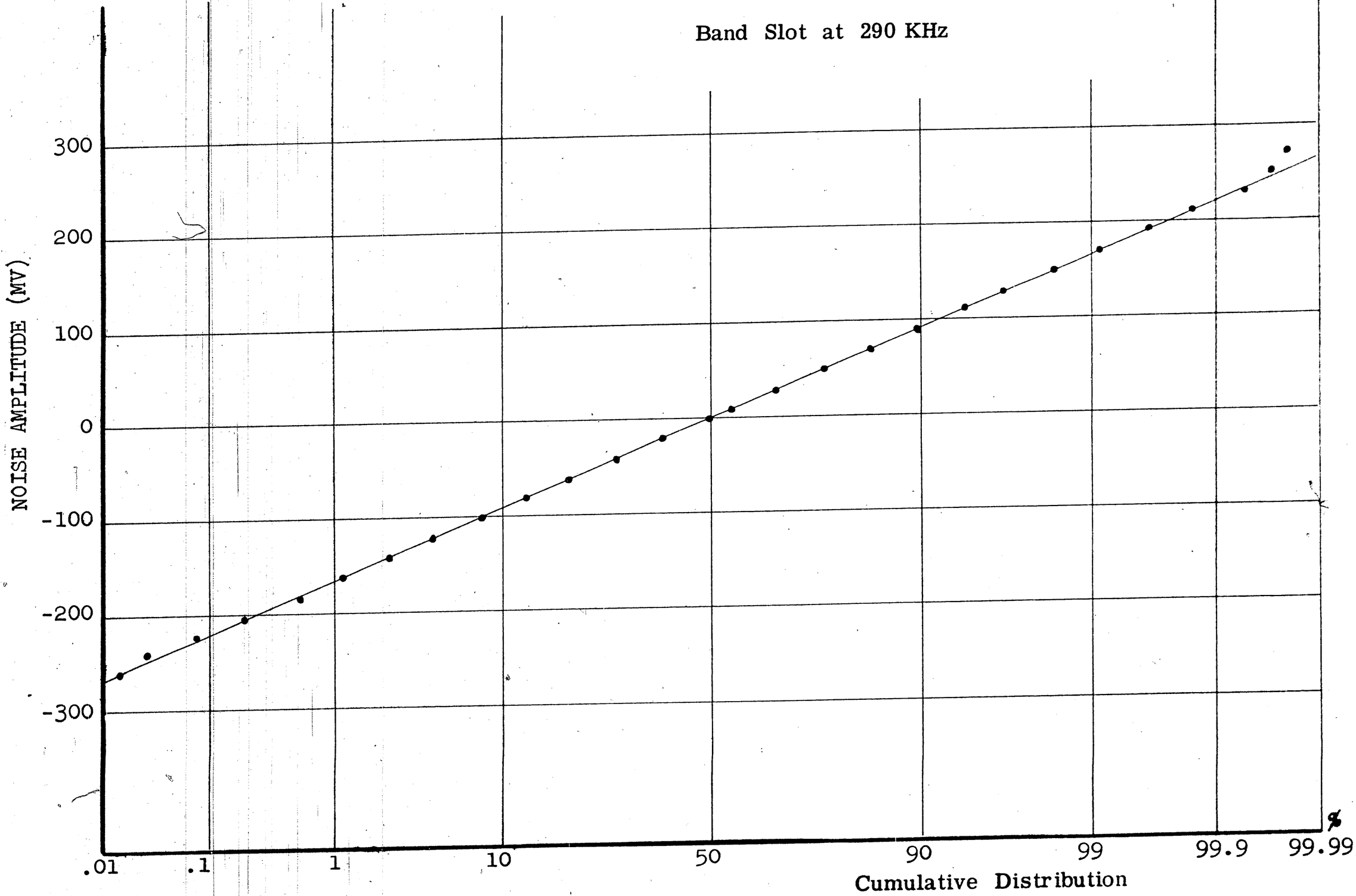


Figure 4.15

## NOISE DISTRIBUTION

C/N = 2 dB

Band Slot at 70 KHz

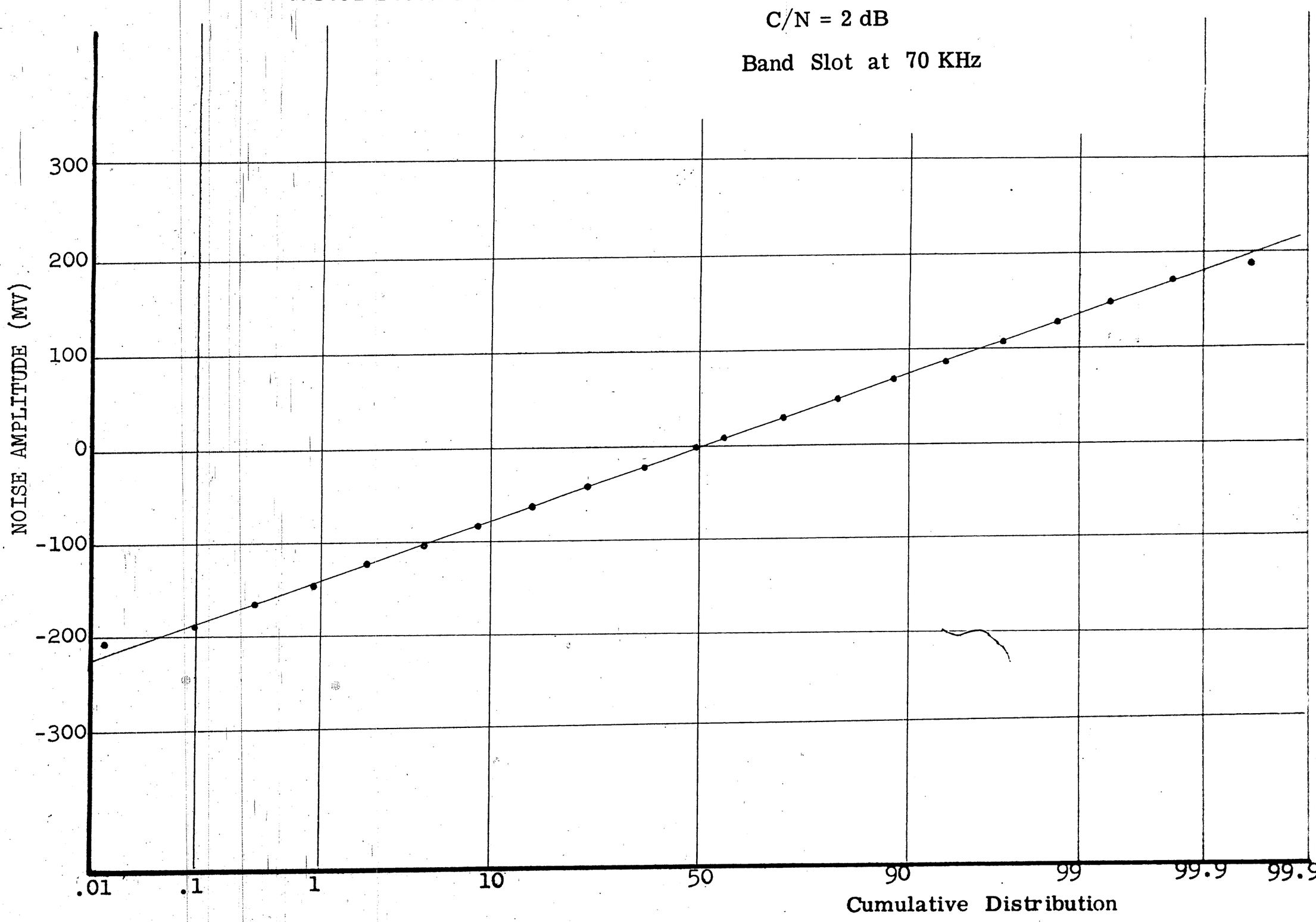


Figure 4.16

## NOISE DISTRIBUTION

C/N = 2 dB

Band Slot at 105 KHz

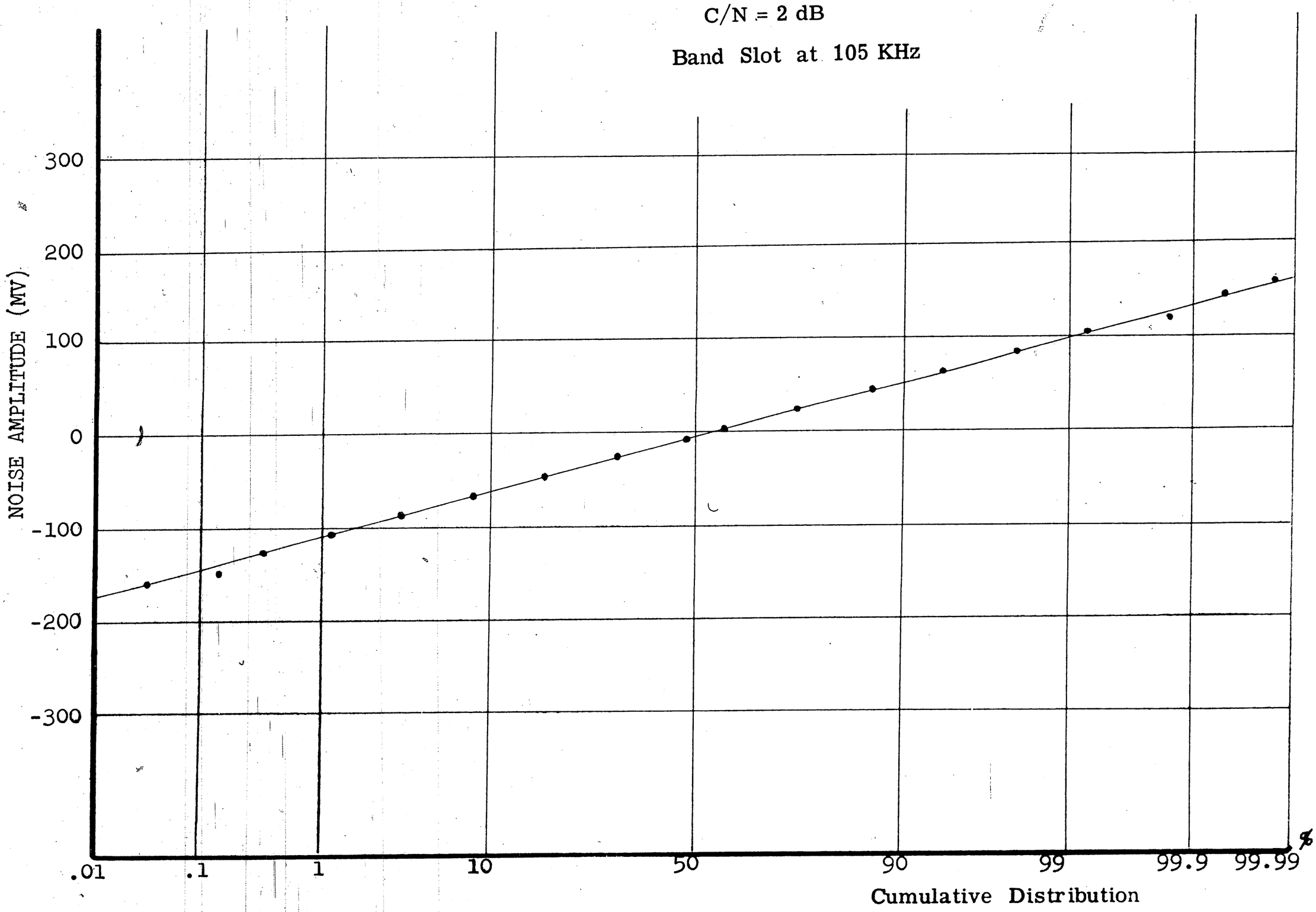


Figure 4.17

## NOISE DISTRIBUTION

C/N = 2 dB

Band Slot at 290 KHz

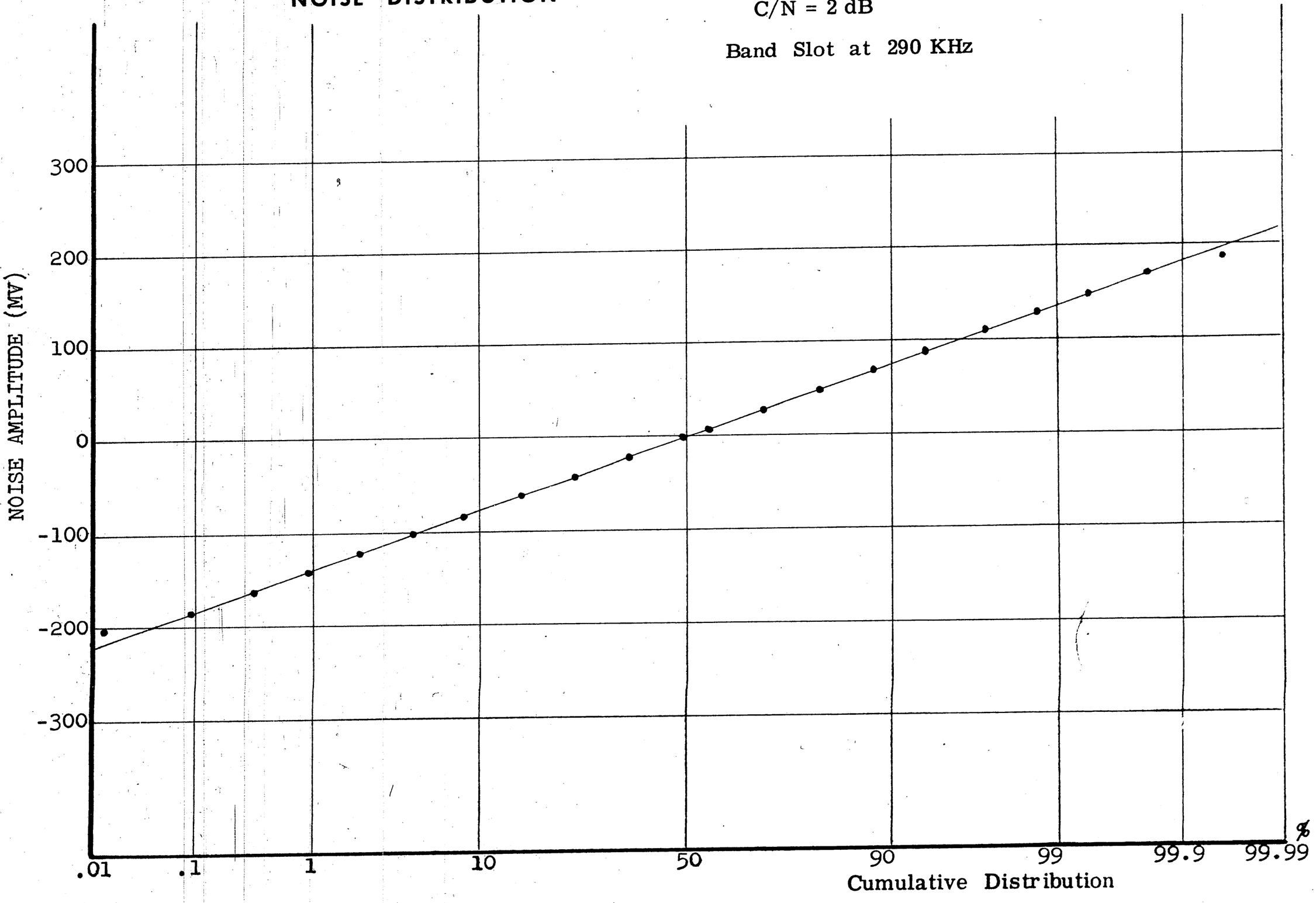


Figure 4.18

## NOISE DISTRIBUTION

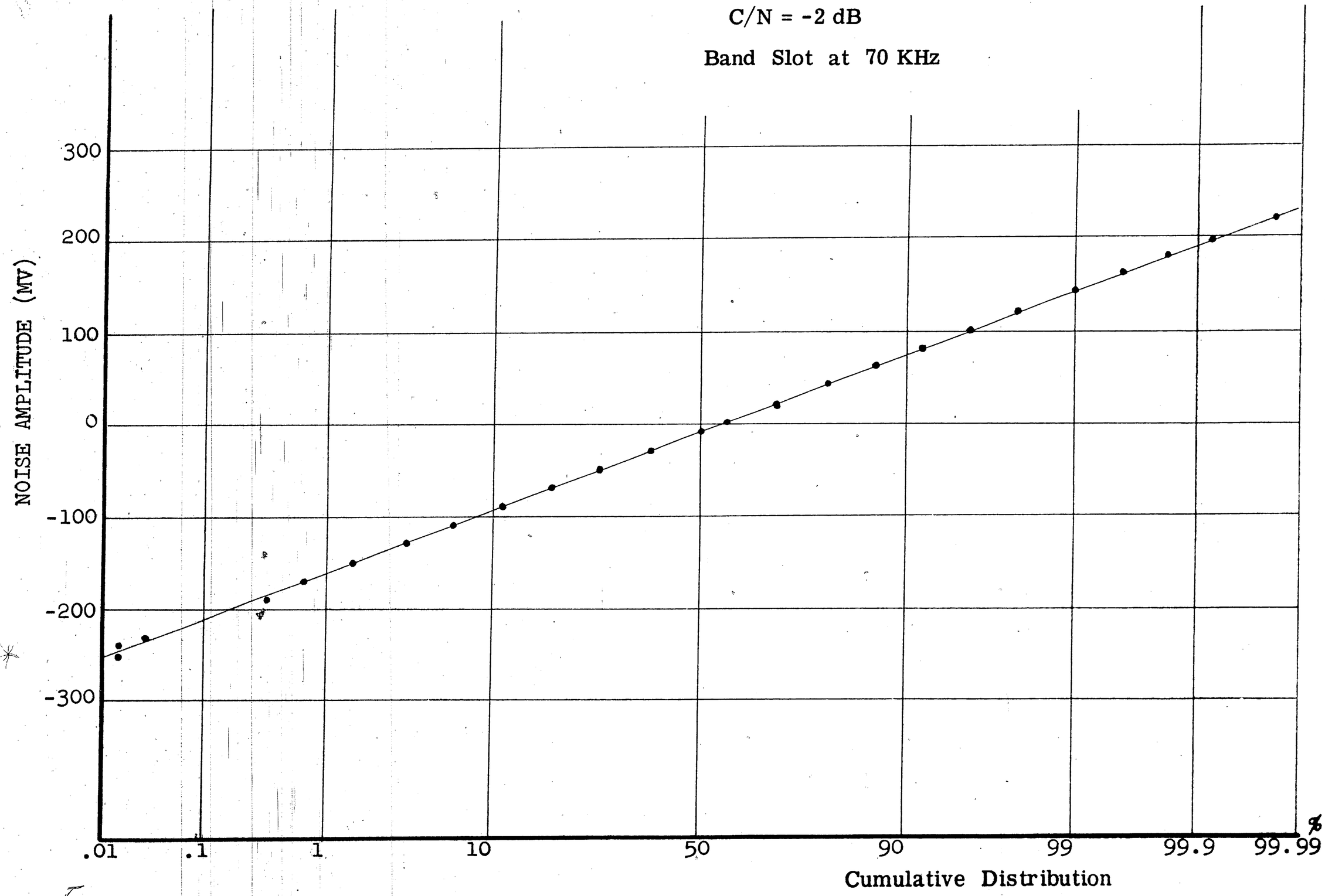


Figure 4.19

## NOISE DISTRIBUTION

C/N = -2 dB

Band Slot at 105 KHz

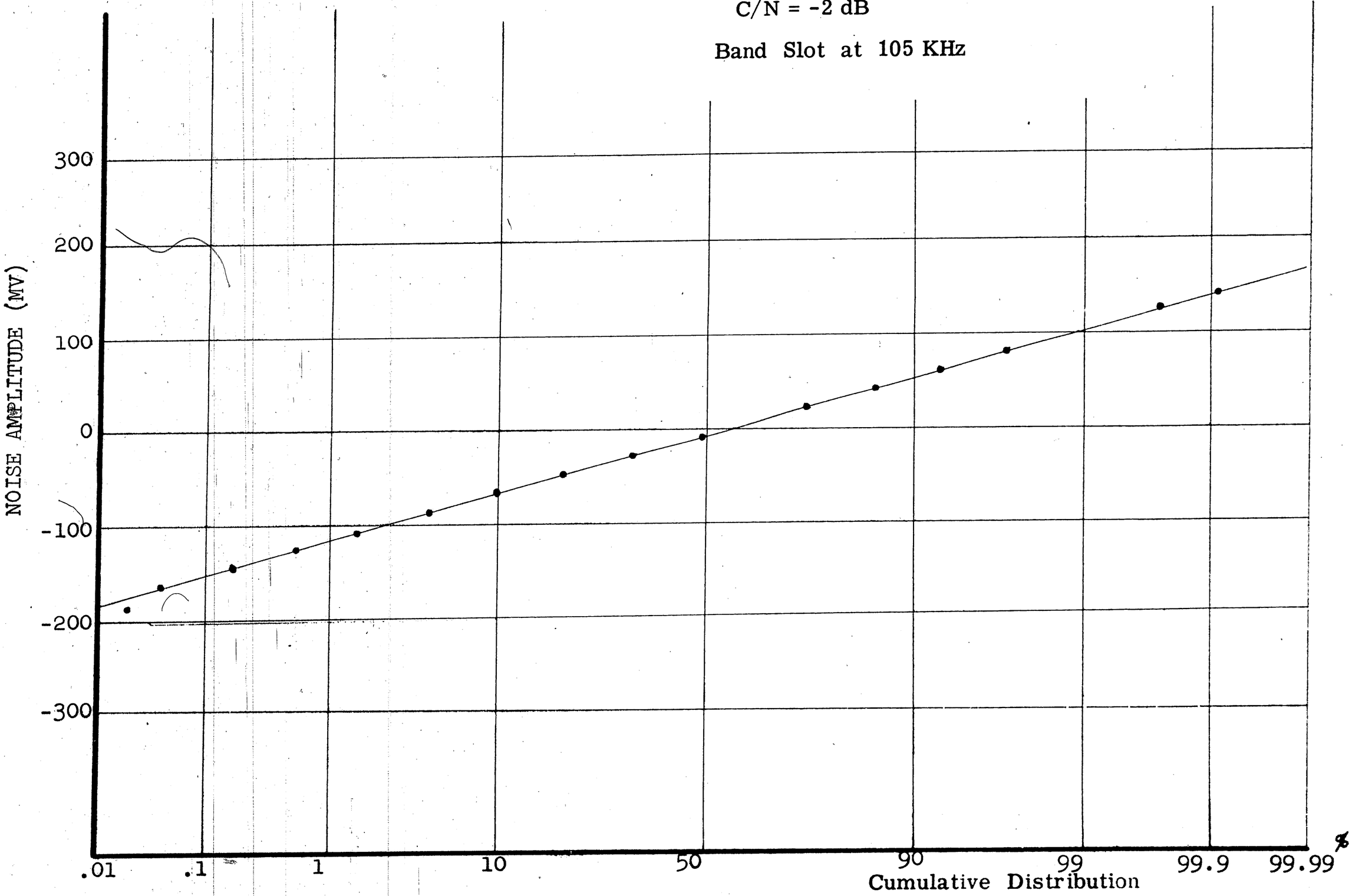


Figure 4.20

## NOISE DISTRIBUTION

C/N = -2 dB

Band Slot at 290 KHz

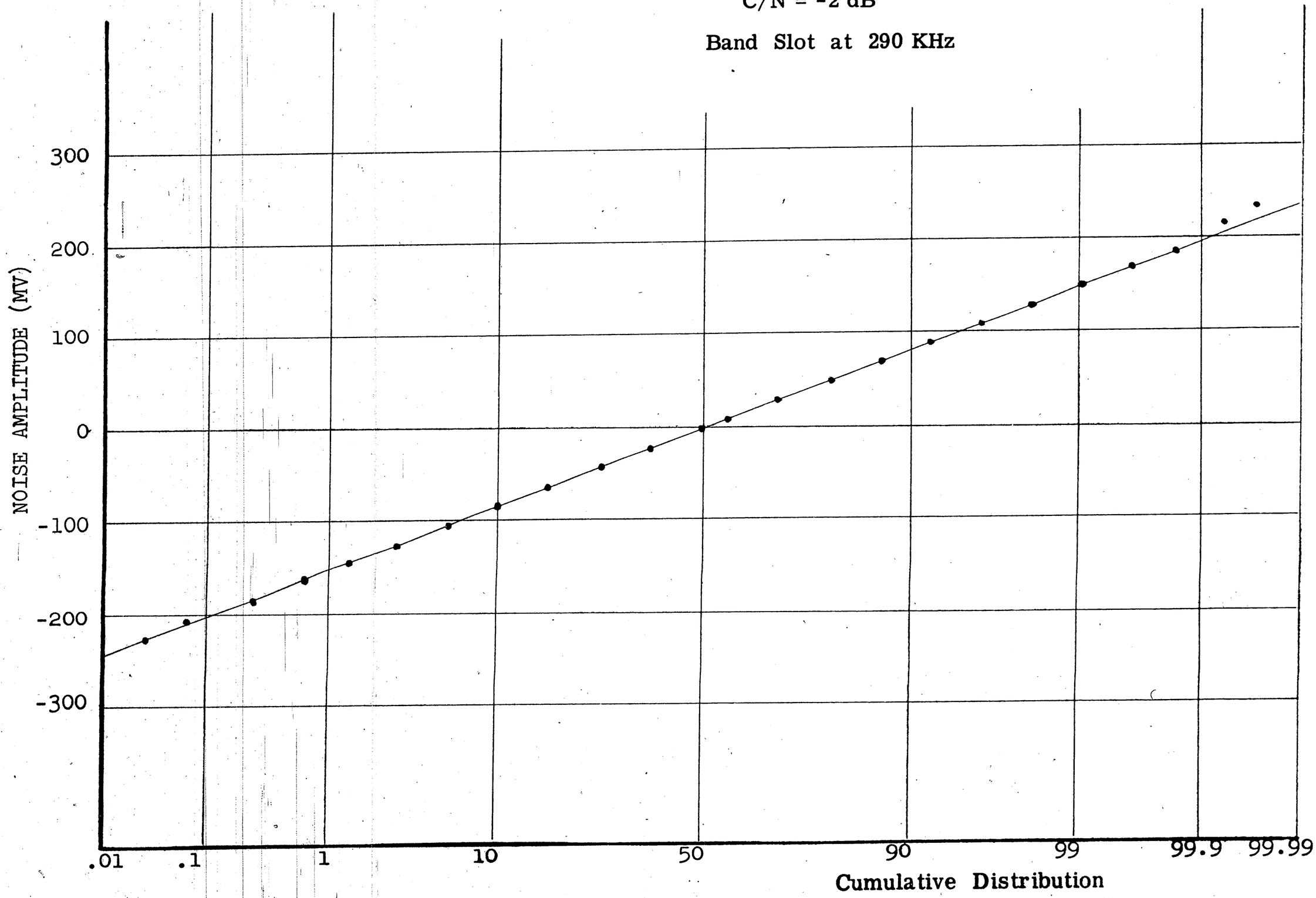


Figure 4.21

## Appendix: Equipment

MUX-DEMUX - Bell Telephone Laboratories, Inc.

The multiplex-demultiplex equipment was developed and constructed at BTL to provide 3 KHz test channels with center frequencies at 70, 105, 290, 534, and 1002 KHz. The performance characteristics are comparable with the standard Bell System type L multiplex equipment.

DEMOD - Radio Engineering Laboratories

REL Type 1094 Receiver, 22770 Demodulator.

The Type 1094 Receiver is designed for use in a forward propagation tropospheric scatter communications system. The demodulator section was used as a receiver at 70MHz (the IF frequency of the tropo receiver).

MOD - Radio Engineering Laboratories

REL Type 1093 Exciter, 22700 Modulator.

The 22700 Modulator was used to provide a 70MHz carrier.

PREAMP - Bell Telephone Laboratories

Developed at BTL for use with the REL equipment described above, the preamplifier has a bandwidth of 10MHz with center frequency at 70MHz and a noise figure of 7.9dB.

OSCILLOSCOPE - Tektronix

Type 585A.

ATTENUATOR - Telonic Industries, Inc.

Model TG-950

1 to 102dB, 50 ohms

RF VOLTMETER - Booton Electronics Corp.

Model 91DA-S5

-58dBm to +23dBm.

ANALOG RECORDER - Viking

Model RP120.

TAPEX SYSTEM -

The equipment inside the dotted line in Fig. (4.1) is part of the TAPEX system developed and constructed at Bell Telephone Laboratories (Murray Hill, N. J.). The system consists of remote digital data stations (including the analog to digital convertor) plus the hardware and software necessary to convert the data to a form suitable for processing. The digital data is stored on magnetic tape for further processing on an IBM 360 computer system at BTL in Holmdel, New Jersey.

## References


1. Armstrong, E. H., "A Method of Reducing Disturbances in Radio Signaling by a System of Frequency Modulation", Proceeding of the I.R.E., Vol. 24 (1936).

2. Crosby, M. G., "Frequency Modulation Noise Characteristics", Proceedings of the I.R.E., Vol. 25 (1937).

3. Middleton, D., "Spectrum of Frequency Modulated Waves after Reception in Random I, II", Quarterly Applied Mathematics, Vol. 7 (1948), Vol. 8 (1950).

4. Rice, S. O., "Statistical Properties of a Sine Wave Plus Random Noise", Bell System Technical Journal, Vol. 27 (1948).

5. Stumpers, F., "Theory of Frequency Modulation Noise", Proceedings of the I.R.E., Vol. 36 (1948).

6. Rice, S. O., "Mathematical Analysis of Random Noise", Bell System Technical Journal, Vol. 23 (1944), Vol. 24 (1945).

7. Sveshnikov, A. A., Applied Methods of the Theory of Random Variables, Pergamon Press Ltd., London, 1966.

8. Downing, J. J., Modulation Systems and Noise, Prentice-Hall, Inc., Englewood Cliffs, New Jersey, 1964.

9. Schwartz, M., Information Transmission, Modulation, and Noise, McGraw-Hill, Inc., New York, 1959.

10. Swartz, M., Bennett, W. R., and Stein, S., Communication Systems and Techniques, McGraw-Hill, New York, 1966.

11. Rice, S. O., "Noise in FM Receivers", Proceedings of the Symposium on Time Series Analysis, Brown University, 1962, edited by M. Rosenblatt.

12. Gnedenko, B. V., The Theory of Probability, Chelsea Publishing Co., New York, 1962.

## Vita

Charles Joseph Ludinsky was born in Buck Mountain, Pennsylvania, on December 15, 1945. He attended the Mahanoy Area public schools, Mahanoy City, Pennsylvania, and was graduated from the college preparatory program in June, 1963. He entered the Pennsylvania State University in September, 1963, and received the degree of Bachelor of Science in Electrical Engineering on June 10, 1967. He enrolled in the Graduate School at Lehigh University in September, 1967.

Mr. Ludinsky is a member of Eta Kappa Nu, Tau Beta Pi, Sigma Tau, and Phi Kappa Phi. He is also a member of the Institute of Electrical and Electronic Engineers and an employee of Bell Telephone Laboratories at Holmdel, New Jersey.